Theoretical analysis of pressure-dependent K_0 for normally consolidated clays using critical state soil models

Nian Hu, PhD
State Key Lab for Geomechanics and Deep Underground Engineering
China University of Mining and Technology, Xuzhou, 221116, China
Nottingham Centre for Geomechanics, Department of Civil Engineering,
The University of Nottingham, Nottingham, NG7 2RD, UK
Email:greaterhu@126.com

Xiang-Yu Shang, Associate Professor
Corresponding author
State Key Lab for Geomechanics and Deep Underground Engineering
China University of Mining and Technology, Xuzhou, 221116, China
Email: xyshang@cumt.edu.cn
Tel: +86(0)51683590666

Hai-Sui Yu, Professor
School of Civil Engineering, University of Leeds, Leeds, LS2 9JT, UK
Email: h.yu@leeds.ac.uk

Abstract

The coefficient of earth pressure at rest (K_0) for normally consolidated clays increases nonlinearly with increasing consolidation pressure towards a steady value under high pressure rather than remaining constant. Analytical expressions for evaluating pressure-dependent K_0 were derived from three representative critical state soil models: Modified Cam-clay model (MCC), Original Cam-clay Model (OCC) and Clay and Sand Model (CASM) proposed by Yu (1998). In formulations, we relaxed a well-adopted assumption that stress ratio is kept constant during 1D compression. It is found that the constant stress ratio, corresponding to the well-adopted assumption, is essentially a limit value of the stress ratio as predicted by MCC and CASM under high pressure during 1D compression. The predicted relation between K_0 and consolidation pressure is significantly affected by critical state stress ratio. Without considering the effect of high pressure, the value of K_0 may be considerably underestimated. The results predicted by the proposed formula based on CASM agree well with experimental data, showing the capability of this formula for predicting pressure-dependent K_0.

Keywords: Clay; Pressure-dependent; Critical state soil models; Coefficient of earth pressure at rest.

Introduction

The coefficient of earth pressure at rest, K_0, as coined by Terzaghi (1920), refers to the ratio of horizontal effective stress to vertical effective stress under the condition of no lateral deformation, the stresses being principal stresses with no shear stress applied to the planes on which these stresses act (Bishop1958; Mesri and Hayat 1993). Since this special condition well represents in-situ stress state of ground, K_0 may be one of the most important parameters in geotechnical engineering. It is widely used in both analysis and design of geotechnical structures related to foundations and excavations (Kamei 1997). As suggested by many standards, e.g. Chinese code for design of coal mine shaft and chamber (GB 50384-2007), it is essential to use K_0 to calculate the at-rest lateral soil pressure based on vertical stresses. Underestimating K_0 and hence lateral loads, may increase the failure risk of a geotechnical design (Army Corps of Engineers 1989; Cui 2003; Li and Li 2005). Additionally, in advanced soil models, e.g. MIT-S1 model (Pestana and Whittle 1999) and E-SCLAY1S model (Sivasithamparam and Castro 2016), K_0 is usually used as a basic material parameter for model calibration. Therefore, accurately evaluating K_0 is of great significance in both theory and application.

In laboratory, K_0 can be measured by one-dimensional (1D) consolidation test which is normally used to simulate the stress path experienced by the deposition process of soils. As comprehensively reviewed by Kamei (1997), K_0 is affected by a number of factors, including effective angle of internal friction, the stress history (or over consolidation ratio) and microstructural anisotropy etc. Results from early research have suggested that the value of K_0 for normally consolidated soils can be recognized as a constant for a specific soil type (Mayne and Kulhawy 1982). This may be reasonable when the applied pressure is in a narrow range. However, over the past two decades, accumulated evidence has demonstrated that K_0 is not generally kept constant, but may vary obviously with consolidation pressure in a wide range for both clays (Ting et al. 1994; Li et al. 2006; Abdulhadi et al. 2012; Yao et al. 2014) and sands (Okochi and Tatsuoka 1984; Yamamuro et al. 1996; Guo 2010). This is not surprising if we are aware of that the fabric of clays change dramatically from low pressure to high pressure during 1D compression (Martin and Ladd 1997). In fact, clays consolidated at high pressures possess a much smaller void ratio and stronger water-clay links than that at low pressures. The traits of stress-strain relation of clay under high pressure differ from those under low pressure: (1) the normal consolidation line (NCL) of clay subjected to a wide range of pressure is bilinear with the slope changing typically at around 0.4-2MPa (Djèran-Maigre et al. 1998; Marcial et al. 2002;Balle et al. 2010 ;Shang et al. 2015a); (2) The slope of critical state line in p-q plane (i.e., critical state stress ratio) decreases with increasing mean effective pressure (Wang and Mao 1980; Graham et al. 1990; Shang et al. 2012; Abdulhadi et al. 2012).

Analytical expressions of K_0 have been proposed for both normally consolidated and over-consolidated soils. In particular, Jaky (1944) theoretically related K_0 to the effective angle of internal friction φ':

$$K_0 = (1 - \sin\varphi')\frac{1+2/3\,\sin\varphi'}{(1+\sin\varphi')} \tag{1}$$

The above equation can be simplified using the following approximation:

$$K_0 = 1 - \sin\varphi' \tag{2}$$

This approximation has been widely adopted in geotechnical engineering (Mayne and Kulhawy 1982; Mesri and Hayat 1993) due to its simplicity with relative accuracy (Wroth, 1972). In

Jaky's equation, φ' is mobilized friction angle and assumed to be a constant. In fact, this angle is not necessarily a constant, especially for soils exhibiting behavior of strain hardening and softening. In practice, both peak value and critical state value of friction angle may be used, e.g., for sands. However, for normally consolidated clay, the critical state friction angle is usually used since no peak friction angle is existent (Mesri and Hayat 1993, Lee et al. 2013). Analytical expressions of K_0 have also been proposed based on the critical state soil models such as Cam-clay models under various assumptions (Schofield and Wroth 1968; Wood 1990; Federico et al. 2009). The assumption that the stress ratio remains constant during 1D compression is well-adopted in the theoretical derivation of K_0. It is worth noting that the decrease in K_0 with increasing critical state friction angle, as featured by Eq. (2), is similar to predictions from critical state models (Schofield and Wroth 1968; Wood 1990; Kamei 1997).

Nonetheless, few attempts have been made in literature to calculate K_0 with incorporating the effect of high pressure using critical state soil models. The aim of this paper is to propose analytical expressions of pressure-dependent K_0 for normally consolidated clays based on three critical state soil models, including Modified Cam-clay model (MCC), Original Cam-clay model (OCC) and Clay and Sand Model (CASM by Yu 1998, 2006). In theoretical derivations, the assumption that stress ratio remains constant was relaxed. The results from the proposed analytical expressions were compared to the numerical results of finite element method (FEM) for verification and experimental tests for validation. We also discussed the variations of K_0 with the compressibility under high pressure and with critical state stress ratio.

Evidence of Pressure-Dependent K_0

Evaluation of K_0 in deep clays has been of particular interest to Chinese geotechnical engineers working in mining engineering for designing mining shaft. Since 1990s, high pressure oedometers (Sui et al. 1994; Li et al. 2006; Wang et al. 2007; Chen 2012) and high pressure triaxial apparatus (Wang et al. 2007; Tian et al. 2009; Xu et al. 2009; Min 2010) have been used to investigate K_0 for undisturbed deep clays (Sui et al. 1994; Li et al. 2006; Wang et al. 2007) and remolded deep clays (Tian et al. 2009; Xu et al. 2009; Min 2010; Chen 2012). The clays employed in these tests were taken from various parts of East China, e.g. Shandong province (Sui et al. 1994; Li et al. 2006; Tian et al. 2009; Xu et al. 2009; Min 2010; Chen 2012) and Hebei province (Wang et al. 2007). Abdulhadi et al. (2012) also reported K_0 tests on resedimented Boston blue clay with the maximum consolidation pressure up to 10 MPa. Results of relation between K_0 and vertical effective stresses σ_v for clays from these tests are presented in Fig.1.

All of these clays, except for the specimen in Chen's test (2012), were normally consolidated clays and the maximum vertical effective stresses applied in tests were larger than 1MPa. It is shown in Fig.1 that in general K_0 for normally consolidated clays increases nonlinearly with increasing pressure and gradually reaches a steady value under high pressure. However, the rate of increase in K_0 and the consolidation pressure at which the value of K_0 becomes steady are different for different clays. The same tendency has been observed for soft remolded kaolinite clay in 1D compression tests even when the maximum consolidation pressure is applied only up to 150kPa (Ting et al.,1994). It should be noted that in Chen's data the sample is pre-consolidated and the lowest value of K_0 corresponds to the pre-consolidated pressure. After this point, it can be taken as normally consolidated sample and an obvious increase in K_0 is observed in sequential compression. A mild increase in K_0 with vertical pressure can be observed from Wang's data (2007). In this case, we may expect that under a lower pressure the increase in K_0 should be remarked and the shown data is in a high pressure range and the corresponding K_0 has already been approaching the steady value. The data from Abdulhadi et al. (2012) can be interpreted in a similar way.

The microscopic mechanism of the above tendency may be reasonably related to the nonlinear development of anisotropic micro-structure in clays during 1D consolidation. X-ray diffraction data (Martin and Ladd 1997) showed that the change in fabric with increasing consolidation pressure is most pronounced with samples at low stresses, while the change in fabric is very small at large stresses. Scanning Electron Microscope (SEM) observation by Li et al. (2006) indicated that the platy clay particles tend to be rearranged gradually from an initially non-parallel state into a parallel stacked state as consolidation pressure increases. In the stacked state the normals of particles coincide with direction of vertical stress. At high pressures, the normals of particles stop changing. The characteristic of fabric evolution of clay particles during 1D compression was also demonstrated by numerical simulations using discrete element method (Anandarajah1994, 2000; Smith et al. 2009; Ferrage et al. 2015) and coarse-grained molecular modelling (Sjoblom 2016). Besides, using the particle-scale numerical simulations in which physicochemical forces between clay particles are considered, Smith et al. (2009) showed that K_0 of a montmorillonite with stacked parallel particles decreases with decreasing face-to-face distance and increasing edge-to-edge distance. The dependency of these distances on consolidation pressure may also result in the pressure-dependency of K_0.

A similar tendency of K_0 has been observed in laboratory test of granular materials like sands. Yamamuro et al. (1996) exhibited that the value of K_0 for a Gypsum sand increases with pressure up to hundreds of megapascals with massive breakage. Results from tests on two granular materials carried out by Guo (2010) revealed that K_0 depends not only on critical state friction angle, but also on void ratio and pressure. The maximum vertical effective stress applied in Guo's tests is less than 800kPa, where the breakage of sand grain is less likely to occur. Micromechanical model (Liou and Pan 2003) and discrete element method (Shin and Santamarina 2009) have been successfully used to capture the experimentally observed relation between K_0 and fabric evolution during 1D compression.

In this paper our aim is to predict the pressure-dependent K_0 from phenomenological models based on critical state concept, which will be presented in the following sections.

Theoretical Analyses

We denote the maximum and minimum effective principal stresses as σ_1 and σ_3, respectively. In triaxial stress state, the effective mean stress p and deviatoric stress q can be expressed by σ_1 and σ_3 as follows:

$$p = (\sigma_1 + 2\sigma_3)/3 \tag{3}$$

$$q = \sigma_1 - \sigma_3 \tag{4}$$

During 1D compression for normally consolidated soils, the vertical effective stress σ_v and horizontal effective stress σ_h equal σ_1 and σ_3, respectively. Using the definition of K_0, it can be related to the stress ratio by

$$K_0 = \frac{\sigma_h}{\sigma_v} = \frac{\sigma_3}{\sigma_1} = \frac{3-\eta}{3+2\eta} \tag{5}$$

where η is the stress ratio defined as

$$\eta = \frac{q}{p} \tag{6}$$

If K_0 varies nonlinearly with pressure, then it is impossible for the stress ratio to remain constant during 1D compression for clays. By differentiating Eq. (6), we generally obtain:

$$dq = pd\eta + \eta dp \tag{7}$$

The assumption of constant stress ratio requires that $d\eta = 0$, and hence there is

$$dq = \eta dp \tag{8}$$

Formulations with assumption of constant ratio

With assuming that elastic shear deformation is negligible and stress ratio does not change with increasing pressure, analytical expression of K_0 was derived by Schofield and Wroth (1968) from energy conservation equation of OCC as follows:

$$K_0 = \frac{6+3\Lambda-2M}{6-6\Lambda+4M}, \text{ M>1.5(1-}\kappa/\lambda) \tag{9}$$

where Λ=(1-κ/λ), λ and κ are the slopes of normal compression line and swelling line in semi-logarithmic compression plane, and M, termed as critical state stress ratio, is the slope of critical state line in the p-q space. M can be linked to critical state friction angle φ_c' through

$$M = \frac{6\sin\varphi_c'}{3-\sin\varphi_c'} \tag{10}$$

By adopting the same assumptions, Schofield and Wroth (1968) showed that the use of MCC leads to a more reasonable K_0 :

$$K_0 = \frac{2-\Psi}{2(1+\Psi)} \tag{11}$$

where $\Psi = \sqrt{\Lambda^2 + \frac{4}{9}M^2} - \Lambda$.

By incorporating the elastic shear strain but still assuming a constant stress ratio, Wood (1990) obtained a cubic equation for determining the stress ratio during 1D compression based on MCC:

$$\frac{\eta_{\mathrm{Knc}}(1+\nu')(1-\Lambda)}{3(1-2\nu')}+\frac{3\Lambda\eta_{\mathrm{Knc}}}{M^2-\eta_{\mathrm{Knc}}{}^2}=1 \tag{12}$$

where ν' is the Poisson's ratio, and η_{Knc} is the stress ratio corresponding to the value of K_0 during 1D compression. The first term at the left-hand side of Eq.(12) can be recognized as the contribution from elastic shear strain. When $\Lambda = 1(\mathrm{i.e.}\,\kappa/\lambda = 0)$, the elastic strain is negligible as compared with the plastic strain. Ignoring the first term, Eq. (12) reduces to

$$\eta_{\mathrm{Knc}}{}^2 + 3\Lambda\eta_{\mathrm{Knc}} - M^2 = 0 \tag{13}$$

The solution of Eq. (13) is that $\eta_{\mathrm{Knc}} = 3\Psi/2$. Eq. (11) is thus obtained by inserting η_{Knc} into Eq. (5). Eq. (12) can be rewritten in the form of cubic equation with respect to η_{Knc} as

$$\Omega(M^2 - \eta_{\mathrm{Knc}}{}^2)\eta_{\mathrm{Knc}} - (M^2 - \eta_{\mathrm{Knc}}{}^2) + 3\Lambda\eta_{\mathrm{Knc}} = 0 \tag{14}$$

where Ω reflects the influence of elastic shear strain, i.e.,

$$\Omega = \frac{(1+v')(1-\Lambda)}{3(1-2v')} \tag{15}$$

It is evident that none of the above formulae takes into consideration the effect of high pressure on K_0. In the formulations of Eqs. (9), (11) and (12) the assumption that stress ratio is kept constant during 1D compression is employed. However, this may not be consistent with experimental observation since, as mentioned above, K_0, hence the stress ratio, is not a constant during the one-dimensional compression of clay under high consolidation pressure. Illustrated as an example, K_0 is derived from MCC by relaxing the assumption of the constant stress ratio in the following section.

Formulation based on MCC

For normally consolidated soils, the response of soils should always be elastic-plastic during 1D compression. Stress-strain relation of MCC can be summarized in an incremental form as follows (Wood 1990):

$$\begin{bmatrix} d\varepsilon_p^{\mathrm{e}} \\ d\varepsilon_q^{\mathrm{e}} \end{bmatrix} = \begin{bmatrix} \frac{\kappa}{vp} & 0 \\ 0 & \frac{2(1+v')}{9(1-2v')}\frac{\kappa}{vp} \end{bmatrix} \begin{bmatrix} dp \\ dq \end{bmatrix} \tag{16}$$

$$\begin{bmatrix} d\varepsilon_p^{\mathrm{p}} \\ d\varepsilon_q^{\mathrm{p}} \end{bmatrix} = \frac{\lambda-\kappa}{vp(M^2+\eta^2)} \begin{bmatrix} M^2-\eta^2 & 2\eta \\ 2\eta & \frac{4\eta^2}{M^2-\eta^2} \end{bmatrix} \begin{bmatrix} dp \\ dq \end{bmatrix} \tag{17}$$

where $d\varepsilon_p^{\mathrm{e}}$ and $d\varepsilon_p^{\mathrm{p}}$ are the elastic and plastic volumetric strain increments; $d\varepsilon_q^{\mathrm{e}}$ and $d\varepsilon_q^{\mathrm{p}}$ are the elastic and plastic shear strain increments; dp and dq are the mean and deviatoric stress increments; and υ=1+e is the specific volume in which e is the void ratio. In case of 1D compression, the strain condition should satisfy:

$$\frac{d\varepsilon_p}{d\varepsilon_q} = \frac{d\varepsilon_p^{\mathrm{e}}+d\varepsilon_p^{\mathrm{p}}}{d\varepsilon_q^{\mathrm{e}}+d\varepsilon_q^{\mathrm{p}}} = \frac{3}{2} \tag{18}$$

where $d\varepsilon_p$ and $d\varepsilon_q$ are the total volumetric and deviatoric strain increments, respectively. With the aid of Eq. (18), together with constitutive equations (16) and (17), eliminating dq in Eq. (7) leads to a relation between the mean effective stress p and the stress ratio η in an incremental form:

$$\frac{dp}{p} = R(\eta)d\eta = \frac{Nu(\eta)}{De(\eta)}d\eta \tag{19}$$

where R(η) represents the integrand, and $Nu(\eta)$ and $De(\eta)$ are denoted, respectively, as the numerator and denominator of integrand R(η):

$$Nu(\eta) = \frac{2\Lambda}{M^2+\eta^2}(M^2-\eta^2-3\eta)\eta - \Omega(M^2-\eta^2) \tag{20}$$

$$De(\eta) = \Omega(M^2-\eta^2)\eta - (M^2-\eta^2) + 3\Lambda\eta \tag{21}$$

Integrating Eq. (19) for a given initial condition gives

$$p = p_0 \mathrm{e}^{\int_{\eta_0}^{\eta} R(\eta)d\eta} \tag{22}$$

where p_0 is the initial mean effective stress and η_0 is the initial stress ratio. Bearing Eq. (5) in mind, the pressure-dependency of K_0 is implied by Eq.(22). As long as material parameters v', Λ and M are known, the integral $\mathrm{e}^{\int_{\eta_0}^{\eta} R(\eta)d\eta}$ on the right-hand side of Eq. (22) can be numerically determined. However, it is instructive to analyze the characteristics of integrand R(η) before performing numerical integration.

Characteristics of the formula

It is interesting to find that the equation De (η) = 0 with respect to η is equivalent to Eq. (14) with respect to η_{Knc} as obtained by Wood (1990). Rearranging Eq. (19) leads to

$$d\eta = \frac{De(\eta)}{Nu(\eta)}\frac{dp}{p} \tag{23}$$

When De (η) approaches zero, the increment of stress ratio,dη, tends to vanish, regardless of increasing p, which means that stress ratio tends to reach a limit value, i.e.η_{Knc} in Eq. (14). If De (η) = 0 is reached, then R (η) in Eq. (19) would be singular and Eq. (22) would be unsolvable. Therefore, the stress ratio η_{Knc} which satisfies Eq. (14) should be a limit value of the stress ratio during 1D compression if MCC is assumed for soil behavior.

Since the stress ratio that satisfies De (η) = 0 significantly affects the solution of Eq. (22), it is necessary to study the roots of equation De (η) = 0.The denominator De (η), which is a cubic function of stress ratio, always has three distinct roots for a wide range of realistic (experimentally observed) values of v', Λ and M, which has been confirmed by our numerous calculations. Figure 2 illustrates typical distribution of roots of De (η) = 0 for a set of typical values of v', Λ and M. As shown in Fig.2, the only reasonable root, η_1 (or η_{Knc}), locates in the interval (0, M). Consequently, the feasible integral interval for Eq. (22) with respect to η is $(\eta_1, \eta_0]$ if $\eta_0 > \eta_1$, or $[\eta_0, \eta_1)$ if $\eta_0 < \eta_1$ where η_0 is the initial stress ratio.

When stress ratio falls into any of the two intervals, the numerator Nu (η) is always negative, and hence R(η) has the opposite sign against De (η). As shown in Fig.2, the denominator De (η) is positive when evaluated in $(\eta_1, \eta_0]$; it is negative when evaluated in $[\eta_0, \eta_1)$. Therefore, the stress ratio will decrease (increase) with increasing mean effective stress if $\eta_0 > \eta_1$ ($\eta_0 < \eta_1$) form Eq. (9). Recalling Eq. (5), K_0 will correspondingly increase (decrease).

Using the solution of cubic equation (e.g. William et al. 1997), the expression of η_1 can be given in closed form:

$$\eta_1 = -2\sqrt{Q}\cos\left(\theta - \frac{2\pi}{3}\right) + \frac{1}{\Omega} \tag{24}$$

where

$$Q = \frac{1}{9\Omega^2} + \frac{\Lambda}{\Omega} + \frac{M^2}{3};\ \ \theta = \arccos\left(\frac{U}{\sqrt{Q^3}}\right);\ \ U = -\frac{1}{27\Omega^3} - \frac{\Lambda}{2\Omega^2} + \frac{M^2}{3\Omega}$$

The influences of parameters M, Λ and v' on limit stress ratio η_1 are presented in Fig.3. It can be seen from Fig. (3) that η_1 increases remarkably as the increasing M for a specific v' and Λ while it only changes slightly over a wide range of v' and Λ for a specific M. This is also confirmed by more numerical calculations using different parameter sets (not showing here). Among them, M has the most significant influence on η_1. It is not surprising if we notice that in Jaky's formula, K_0 is only affected by friction angle, and hence the corresponding η_1 is essentially dependent only on M by considering the relationship between M and critical state friction angle, i.e. Eq. (10). By comparing the differences between Eqs. (12) and (14), Poisson's ratio v' and parameter Λ actually reflect the effect of elastic strain on limit stress ratio, which is the reason why they are insensitive to η_1 as compared with M.

Recalling that critical state stress ratio M under high pressure is normally lower than that under low pressure, it can be inferred that η_1 should be lower under high pressure. For normally consolidated clay, critical state friction angle φ_c' can be used as φ' in Jaky's formula in Eq. (2). And critical state stress ratio M can be linked to φ_c' in Eq. (10). By employing Eqs. (5) and (10), we can rewrite Jaky's formula as follows:

$$\eta_1 = \eta_{Knc} = \frac{3M}{6-M} \tag{25}$$

From this relation, it can be seen that M increases monotonically with η_1, which is consistent with the tendency shown in Fig 3.a.

Results based on MCC

Verification and Validation

Although some results of K_0 for clays under high pressure were reported as presented in Fig.1, there have been few experimental studies on the critical state behavior of clayey soils under high pressure. This may be due to the huge challenge for conventional laboratory shear devices to perform high pressure triaxial tests on clayey soils. A series of triaxial tests on a remolded deep clay which is also used by Min (2010), subjected to a wide range of consolidation pressures, were carried out to investigate its critical state mechanical properties (Shang et al. 2015b). Therefore, experimental data of Min (2010) shown in Fig.1 were chosen to validate the solution of Eq. (22). Material parameters of the remolded deep clay relevant to MCC were calibrated (Shang et al. 2015b) from these tests as follows: λ=0.093, k=0.023 and M=0.99 (applicable to normal pressure less than 2MPa) or 0.447 (applicable to high pressure greater than 2MPa), respectively. In addition, the value of the Poisson's ratio υ' was estimated to be 0.26 which can be used to give a reasonable FEM simulation of pre-yield behavior based on a critical state model (Shang 2009). Take the start point on the Min's curve in Fig.1 as the initial state at which η_0 is 0.381 and p_0 is 1.565 MPa.

Note that the relation between K_0 and σ_v can be established by combining Eq. (22) with Eqs. (3) and (5). As Eq. (22) cannot be analytically integrated, a simple numerical technique is used to calculate the solution, which is verified by results of finite element simulation. FEM simulation was performed in ABAQUS (2013), a well-known commercial finite element package, using an axial symmetric four-node reduced integration element CAX4R (shown in Fig.4) and extended Cam-clay model. The nodes at the bottom are vertically fixed, and all the nodes are laterally fixed. Through these constraints, only vertical deformation is allowed in the element, so that 1D compression is properly modelled.

The yield function of extended Cam-clay model in ABAQUS is

$$f(p,t,a) = \frac{1}{\beta^2}\left(\frac{p}{\alpha} - 1\right)^2 + \left(\frac{t}{M\alpha}\right)^2 - 1 = 0 \tag{26}$$

where

$$p = \frac{\mathrm{I}_1}{3} = \frac{\sigma_1+\sigma_2+\sigma_3}{3};\ \ t = \frac{q}{2}\left[1 + \frac{1}{K} - \left(1 - \frac{1}{K}\right)\left(\frac{\bar{r}}{q}\right)^3\right];$$

$$q = \sqrt{3\left(I_2 - \frac{\mathrm{I}_1{}^2}{6}\right)} = \sqrt{\frac{1}{2}[(\sigma_1-\sigma_2)^2 + (\sigma_1-\sigma_3)^2 + (\sigma_2-\sigma_3)^2]};$$

$$\bar{r} = \left(\frac{27}{2}I_3 - 9I_1I_2 + I_1{}^3\right)^{1/3}$$

in which I_1, I_2, I_3 are the first, second and third stress invariants, respectively; p and q are mean effective stress and deviatoric stress in general stress state and can be naturally reduced to those defined in Eqs. (3) and (4) in triaxial stress state respectively. β is a constant used to control the shape of the yield surface on the "wet" side of the critical state; α is a hardening variable which defines the size of the yield surface; and K is a constant used to modify the shape of the yield surface in the deviatoric plane. In this study, β and K were both set to be 1 so that the yield surface of the extended Cam-clay model reduces to that of MCC. Like MCC, associated flow rule and volume hardening rule originated from normal compression line were also adopted in ABAQUS. In addition, the poroelastic model in ABAQUS was used, which leads to the same elastic stress-strain relation as that presented in Eq. (16) as long as the assumption of small deformation holds true. More details are referred to the documentation of ABAQUS (2013). Theoretically, the solution of Eq. (22) which is derived from MCC should agree exactly with that from the FEM simulation.

It is evident from Fig.4 that the analytical solutions are closely consistent with the FEM simulation so that the numerical integration of Eq. (22) is verified. Through the comparisons in Fig.4, Eq. (22) based on MCC is capable of predicting the general tendency of nonlinear increase in K_0 with increasing pressure towards a steady value, which may be attributed to the relaxation of the assumption of constant stress ratio. The significant influence of M on the steady value of K_0 is also shown in Fig.4. In particular, a lower M, corresponding to a high pressure, contributes to a rapider increase in K_0. The use of critical state stress ratio at low pressures (M=0.99) may largely underestimate K_0 at high pressures, although a similar tendency can be observed.

Critical state stress ratio M represents the average (or macroscopic) internal friction coefficient of a clay. In fact, as an intrinsic variable at constant volume, it has a very close relationship with the friction coefficient between particles in a granular material (Bolton 1986; Lee et al. 2013). For a clay, it can characterize the degree of difficulty of the relative movement between two clay particles. During 1D compression, clay particle tends to align in the same direction as the increase of pressure. Under high pressure, the orientation of clay particle becomes almost identical, which may form the microscopic fabric underlying a steady value of K_0. Friction coefficient is a key factor controlling the movement of clay particle during this process. The greater the friction coefficient is, the more difficult clay particle reorganizes into an order stack. This may be the physical orientation for which the value of K_0 is affected by critical state stress ratio.

When M=0.447 the steady value of K_0 is slightly over-predicted as compared to test data, which is consistent with what reported by Federico et al. (2009). However, there still is a large gap between experimental results and theoretical prediction especially before the steady value is reached, as shown in Fig.4. This large gap may be caused by the yield surface used in MCC, which is not applicable to model clay behavior under high pressure.

Clay behavior under high pressure

The behavior of normally consolidated clay is discussed based on the results from MCC. Figure 5 presents the stress paths in the p-q plane during 1D compression up to a high pressure from different initial stress states on yield surface. In particular, initial state A represents the initial stress state of the sample testes by Min (2010), while the initial state B represents an isotropic stress state. All the initial stress states are reasonably assumed in yield as normally consolidated clays are concerned. It can be seen that whether the initial stress ratio η_0 is larger than the limit stress ratio η_1 or not, stress paths in the p-q plane obtained from the MCC during 1D compression, will gradually move to the line with a slope of $\eta=\eta_1$. Hence, under high pressure the stress ratio predicted by MCC will gradually approach the limit stress ratio independent of the initial stress ratio. It should be noted that when the initial stress ratio is smaller than the limit stress ratio, the value of K_0 gradually decreases to the steady value corresponding to the limit stress ratio.

Figure 6 presents the compression curves in the v-lnp plane corresponding to stress ratios η_0 and η_1 for the results obtained from both the FEM simulation and state boundary surface of MCC. The lines with circular markers in Figs.6 (a) and (b) are compression lines calculated from FEM simulation from two different initial stress states, i.e., A and B in Fig.5. It is evident in Fig.6 that the calculated compression curve is not a straight line over a wide range of pressures, but transfers from K_0 normal compression line (K_0 NCL) for initial stress ratio η_0 to that for the limit stress ratio η_1. In particular, in the case of that $\eta_0 > \eta_1$, the simulated compression curve in Fig. 6(b) shows that the clay under a higher pressure turns out to be slightly less compressible. This is qualitatively consistent with the observation from the experimental compression curves of remolded clays under high pressure (Djèran-Maigre et al. 1998, Shang et al. 2015b).

Analyses based on OCC and CASM

Formulations

Similar analyses were carried out on the basis of OCC and CASM (Yu 1998, 2006). For brevity, only key results are presented with omitting the derivation. For OCC, R(η) in Eq. (22) should be replaced as follows:

$$R(\eta) = \frac{\frac{\Lambda}{M}\left(M-\eta-\frac{3}{2}\right)-\Omega(M-\eta)}{\Omega(M-\eta)\eta-(M-\eta)+\frac{3}{2}\Lambda} \tag{27}$$

with

$$De(\eta) = \Omega(M-\eta)\eta - (M-\eta) + \frac{3}{2}\Lambda \tag{28}$$

CASM was proposed on the basis of the state parameter concept proposed by Been and Jefferies (1985). It is applicable to both sand and clay. CASM and MCC use the same elastic model and hardening rule, but differ in yield surface and flow rule. The yiled surface in CASM can be written as

$$\left(\frac{q}{Mp}\right)^n + \frac{\ln(p/p_r)}{\ln(r)} = 0 \tag{29}$$

where n is a material constant used to modify the shape of the state boundary surface (Yu 1998), r is the spacing ratio defining the distance between the critical state line and the normal consolidation line (NCL) in semi-logarithmic compression plane, and p_r is reference consolidation pressure which controlling the size of yield surface. r and n are newly-introduced material parameters in addition to those of MCC. With n=1 and r=e=2.718, yield surface of OCC is exactly recovered from Eq. (29). Figure 7 illustrates the yield surfaces of MCC, OCC and CASM for M=0.99 and M=0.447. It can be seen the spacing ratio r also controls the ratio between p at critical state and p_r (note that r=2 for MCC). Under high pressure (corresponding to M=0.447), the yield surface is much smaller in the normalized p-q plane.

The original CASM (1998) adopted Rowe's stress-dilatancy relation:

$$\frac{d\varepsilon_p^{\mathrm{p}}}{d\varepsilon_q^{\mathrm{p}}} = \frac{9(M-\eta)}{3M-2M\eta+9} \tag{30}$$

However, it was shown to be unrealistic for stress paths with lower stress ratios, e.g. in case of 1D compression (Yu 2006, P108). Our calculation also showed that the root of the denominator of R(η) obtained from the original CASM is much larger than M. In order to overcome this disadvantage, Yu (2006) proposed a general stress-dilatancy relation as follows:

$$\frac{d\varepsilon_p^{\mathrm{p}}}{d\varepsilon_q^{\mathrm{p}}} = \frac{M^n-\eta^n}{m\eta^{n-1}} \tag{31}$$

Genearally, m may be treated as a material constant. When n=1 and m=1, Eq. (31) reduces to the plastic flow rule of OCC. By setting n=2 and m=2, Eq. (31) reduces to the plastic flow rule of MCC.

By replacing stress-dilatancy relation in Eq. (30) by Eq. (31), the incremental elastic and plastic stress-strain relations of CASM can be summarized as follows

$$\begin{bmatrix} d\varepsilon_p^{\mathrm{e}} \\ d\varepsilon_q^{\mathrm{e}} \end{bmatrix} = \begin{bmatrix} \frac{\kappa}{vp} & 0 \\ 0 & \frac{2(1+v')}{9(1-2v')}\frac{\kappa}{vp} \end{bmatrix} \begin{bmatrix} dp \\ dq \end{bmatrix} \tag{32}$$

$$\begin{bmatrix} d\varepsilon_p^{\mathrm{p}} \\ d\varepsilon_q^{\mathrm{p}} \end{bmatrix} = \frac{(\lambda-\kappa)\ln r}{vp} \begin{bmatrix} \left(\frac{1}{\ln r} - \frac{n}{M^n}\eta^n\right) & \frac{n}{M^n}\eta^{n-1} \\ \left(\frac{1}{\ln r} - \frac{n}{M^n}\eta^n\right)\frac{m\eta^{n-1}}{M^n-\eta^n} & \frac{n}{M^n}\eta^{n-1}\frac{m\eta^{n-1}}{M^n-\eta^n} \end{bmatrix} \begin{bmatrix} dp \\ dq \end{bmatrix} \tag{33}$$

Following the similar procedure for obtaining Eq. (19), R(η) for CASM with stress-dilatancy relation in Eq. (31) is obtained as

$$R(\eta) = \frac{\Lambda \ln r \frac{n}{M^n}\eta^{n-1}\left(M^n - \eta^n - \frac{3m}{2}\eta^{n-1}\right) - \Omega(M^n - \eta^n)}{\Omega(M^n - \eta^n)\eta - (M^n - \eta^n) + \frac{3}{2}\Lambda m \eta^{n-1}} \tag{34}$$

And there is

$$De(\eta) = \Omega(M^n - \eta^n)\eta - (M^n - \eta^n) + \frac{3}{2}\Lambda m \eta^{n-1} \tag{35}$$

With n=1 and m=1 and r=e=2.718, OCC is exactly recovered from CASM. As a result, it is not surprising that Eq. (34) reduces to $R(\eta)$ of OCC. With n=2 and m=2, $De(\eta)$of MCC is recovered from Eq. (35) as CASM and MCC are the same in flow rule and elastic model and hardening law. This means that CASM with n=2 and m=2 can predict the same limit stress ratio as that of MCC under high pressure. Again, v' and Λ reflect the effect of elastic strain on limit stress ratio in Eq. (35). Similar to the case in MCC, the limit stress ratio determined by Eq. (35) is mostly affected by M among the three parameters M, Λ and v'.

Comparisons

Figure 8 presents the variation of K_0 against vertical pressure calculated from OCC. The predicted curves for M=0.447 and M=0.99 both deviate remarkably from the test result. The predicted K_0 does not become steady even under a very high pressure, and the steady value of K_0 predicted from OCC is too high to be rational. This is because the limit stress ratios under high pressure, i.e. roots of the denominator in Eq. (28) for both M=0.447 and M=0.99, are negative, which is shown in Fig.9. The integral interval for R(η)=0 in Eq. (27) is (η_1, η_0). Note that η=0 corresponds to K_0=1. When stress ratio becomes negative, q is negative. In the case, the vertical stress is smaller than the lateral stress and K_0 is larger than 1. As a result, K_0 cannot approach to a steady value less than 1. Obviously, the prediction is not supported by the experimental results shown in Fig.1. From the above discussion, it can be drawn that OCC is not a suitable model for predicting K_0 under high pressure.

Figure 10 presents the calculated K_0 based on CASM for various values of r and M with m=n=2. We intentionally set m=n=2 to compare formula from CASM with that from MCC. In case of m=n=2 the denominators obtained from CASM and MCC are the same so that the steady values of K_0 under high pressure are also identical for a specific M. Clearly, the steady value of K_0 is independent of r, because r is not involved in Eq. (35). A larger r implies a faster increase in K_0 with increasing vertical pressure. Again, the steady value of K_0 is greatly affected by M. Prediction of K_0 using M at a low pressure (e.g., M=0.99) can largely underestimate the value of K_0. In general, M affects the steady value under high pressure while r affects the rate of approaching the steady value. K_0 calculated from CASM with r=2 is almost the same as that from MCC because in this case CASM is almost reduced to MCC. When r = 5.7, the theoretical prediction of corresponding stress path is very close with the test counterpart, as shown in Fig.11.

Recently, Federico et al. (2009) also predicted K_0 of normally consolidated clays using an isotropic critical state model with the same yield surface of MCC but a non-associated potential surface. It was found that the potential surface has an influence on steady value of K_0, which is consistent with our calculations. More specifically, when the same value of M is used in calculations, the steady values of K_0 predicted by OCC are obviously different from those by MCC and CASM (n=2 and m=2). It turns to be more interesting if we notice that MCC and CASM (n=2 and m=2) with different yield surfaces predicted the same steady values. However, in their formulations (Federico et al. 2009) the effect of high pressure on critical state stress ratio was ignored and the assumption of constant stress ratio was employed, therefore, only steady value of K_0 can be obtained.

Sivasithamparam and Castro (2016) discussed the prediction of K_0 based on an anisotropic soil model named as E-SCLAY1S.The model is extended from an anisotropic MCC-type model S-CLAY, proposed by Wheeler et al. (2003), by introducing a new parameter (contractancy parameter) to control the shape of yield surface and plastic potential surface. Similar as that in S-CLAY, anisotropy behavior is represented by the inclination of a distorted yield surface and a rotational hardening law to model anisotropy evolution. Using the model, K_0 can be linked to critical state stress ratio, inclination of yield surface (anisotropy parameter) and contractancy parameter. It is noted that in their derivation both elastic volumetric and shear strains were ignored, and hence only steady value of K_0 can be obtained. As pointed out by Sivasithamparam and Castro (2016), when soil anisotropy is deactivated (i.e., anisotropy parameter is not involved) in the prediction, the contractancy parameter provides an additional degree of freedom to perfectly fit the desired K_0 and the prediction gives similar values to Jaky's formula in Eq.(2) when a suitable value of contractancy parameter is chosen. Once soil anisotropy is involved in the prediction, anisotropy parameter can provide another degree of freedom to fit $K_{0.}$ However, the problem of introducing anisotropy in practical calculation is that it is difficult to determine the initial inclination of the yield surface due to the lack of enough data. Therefore, their formulation is more effective for calibrating model parameters (e.g., initial inclination of yield surface) by fitting a known K_0 rather than for predicting steady value of K_0.

Concluding remarks

From the above discussions, the following conclusions can be drawn:

(a) The value of K_0 increases with increasing consolidation pressure towards a steady value under high pressure. This tendency may be caused by the dramatic evolution of clay fabric at a microscopic scale.

(b) It is essential to use a lower critical state stress ratio for calculating K_0 under high pressure using critical state soil models. Ignoring the effect of high pressure may lead to a severe underestimation of the calculated K_0, which may result in underestimating the lateral loads and greatly increasing the failure risk of a geotechnical design.

(c) The assumption that stress ratio during 1D compression is kept constant (e.g. Wood 1990) may be not applicable to the situation that a remolded clay experiences a wide range of consolidation pressure. When this assumption is relaxed, the derived formula of K_0 based on MCC is shown to be capable of predicting the general tendency of nonlinear increase in K_0. The predicted K_0 based on CASM with r=5.7 shows good agreement with experimental results.

(d) For both the predictions from MCC and CASM with suitable values of n and m, the stress ratio during 1D compression will gradually reach a limit stress ratio, which corresponds to the steady value of K_0 under high pressure. This limit value is equal to the stress ratio obtained using the assumption of constant stress ratio, and is independent of the initial stress ratio. Among the widely-used material parameters, i.e. ν', Λ and M, M has the most significant influence on limit stress ratio (see Fig.3), hence on steady value of K_0.

The proposed equation for K_0 based on CASM has potential applications in calculating lateral loads of mining shaft and shaft friction of pile foundations in deep soils subjected to vertical loading. It should be noted that our discussions are restricted to normally consolidated clays and hence over-consolidated clays are beyond the scope of this paper. However, in many cases an overconsolidated clay will become normally consolidated again under high pressure. Although K_0 of sands also show a tendency of pressure-dependency, the underlying mechanism of this tendency for sands is probably different from that for clays. Further investigations are required for predicting K_0 of over-consolidated clays and sands.

Acknowledgements

The authors gratefully acknowledge the financial support provided by Fundamental Research Funds for the Central Universities (2017XKQY052). The authors would also like to thank the anonymous reviewers for valuable suggestions.

Notation

The following symbols are used in this paper:

K_0	=coefficient of earth pressure at rest;
φ'	=effective angle of internal friction;
φ_c'	=critical state friction angle;
σ_h	=horizontal effective stress; kPa
σ_v	=vertical effective stress; kPa
M	=critical state stress ratio;
m, n	=material constants in CASM;

p = mean effective stress; kPa

q =deviatoric stress; kPa

δp =mean effective stress increment; kPa

δq =deviatoric stress increment; kPa

p_0 =initial mean effective stress; kPa

p_r =reference consolidation pressure; kPa

$R(\eta)$ =integrand appeared in solution;

$De(\eta)$ =denominator of $R(\eta)$;

$Nu(\eta)$ =nominator of $R(\eta)$;

r =spacing ratio defined in CASM;

α,t,$\bar{r}$ =variables related to extended Cam-clay model in ABAQUS; kPa

K, β =parameters related to extended Cam-clay model in ABAQUS;

Q,Θ,U = variables for calculating the limit stress ratio;

$\delta\varepsilon_p^e$ =elastic volumetric strain increment;

$\delta\varepsilon_p^p$ =plastic volumetric strain increment;

$\delta\varepsilon_q^e$ =elastic shear strain increment;

$\delta\varepsilon_q^p$ =plastic shear strain increment;

λ =slope of compression line in semi-logarithmic compression plane;

κ =slope of unloading-reloading in semi-logarithmic compression plane;

v =specific volume;

e =void ratio;

v' =Poisson's ratio;

η =stress ratio;

η_0 =initial stress ratio;

η_1 =limit stress ratio;

η_{Knc} =stress ratio corresponding to K_0;

Λ =1-κ/λ;and

Ω =$(1+v')(1-\Lambda)/3(1-2v')$.

References

Abaqus. (2013). Abaqus 6.13 Documentation: Theory Guide.

Abdulhadi, N.O., Germaine, J.T. and Whittle, A.J. (2012). "Stress-dependent behavior of saturated clay." Canadian Geotechnical Journal, **49**(8), 907-916.

Anandarajah, A. (1994). “Discrete-element method for simulating behavior of cohesive soil.” Journal of Geotechnical Engineering, 120(9): 1593-1613.

Anandarajah, A. (2000). “Numerical simulation of one-dimensional behaviour of a kaolinite.” Géotechnique, 50(5), 509–519.

Army Corps of Engineers. (1989). “Engineering and Design - Retaining and Flood Walls”, Publication Number: EM 1110-2-2502.

Baille, W., Tripathy, S., Schanz, T. (2010). “Swelling pressures and one-dimensional compressibility behaviour of bentonite at large pressures.” Applied Clay Science, **48**(3):325-633.

Been, K and Jefferies, M.G. (1985). “A state parameter for sands”. Géotechnique, **35**, 99-112.

Bishop, A.W., (1958), “Test Requirements for Measuring the Coefficient of Earth Pressure at Rest”, Proceedings, Brussels Conference on Earth Pressure Problems, Vol (1), 2-14.

Bolton, M.D. (1986).The strength and dilatancy of sands. Géotechnique **36**(1), 65–78.

Chen, G.Q. (2012).Study on mechanical properties of K_0 for normally consolidated clays under high pressure and long time when lateral uninstalling. MS Dissertation, China University of Mining and Technology: China; (in Chinese).

Cui, G.X. (2003). “Loading of shaft lining for deep alluvium.” China Journal of Geotechnical Engineering, **25**(3), 294-298 (in Chinese).

Djèran-Maigre, I., Tessier, D., Grunberger, D., Velde, B. and Vasseur, G. (1998). “Evolution of microstructures and of macroscopic properties of some clays during experimental compaction.” Marine and Petroleum Geology; **15**,109-128.

Federico, A., Elia, G., Murianni, A. (2009). “The at-rest earth pressure coefficient prediction using simple elasto-plastic constitutive models." Computers and Geotechnics, **36**, 187－198.

Ferrage, E., Hubert, F., Tertre, E., Delville, A., Michot, L.J. and Levitz, P. (2015). "Modeling the arrangement of particles in natural swelling-clay porous media using three-dimensional packing of elliptic disks." Physical Review E, **91**, 062210.

Graham, J., Saadat, F. and Gray, M.N. (1990). "High-pressure triaxial testing on the Canadian reference buffer material." Engineering Geology, **28**, 391-403.

Guo, P.J. (2010). "Effect of density and compressibility on K_0 of cohesionless soils." Acta Geotechnica, **5**, 225-238.

Jaky, J. (1944). "The coefficient of earth pressure at rest." Journal for Society of Hungarian Architects and Engineers, **78**(22), 355-358 (in Hungarian).

Kamei, Takeshi (1997), "Simplified procedure for evaluating the coefficient of earth pressure at rest." Memoirs of the Faculty of Science & Engineering Shimane University, Series A, **30**, 39-54.

Lee, J., Yun, T.S., Lee, D., Lee, J. (2013). "Assessment of K_0 correlation to strength for granular materials" Soils and Foundations. **53**(4), 584-595.

Li, W.P. and Li, X.Q. (2005). "Mechanism of rupture of shaft linings in coal mine areas buried by thick over-soils in East China." Géotechnique, **55**(3), 237-244.

Li, W.P., Zhang, Z., Sun, R.H., Wang, W.L. and Li, X.Q. (2006). "High pressure K_0 creep experiment and the anisotropy of microstructure of deep buried clay." China Journal of Geotechnical Engineering, **28**(10), 1185-1190 (in Chinese).

Liou, J.C. and Pan, Y.W. (2003). "Fabric evolution of granular assembly under K_0

loading/unloading.” International Journal for Numerical and Analytical Methods in Geomechanics, **27**, 1099-1122.

Marcial, D., Delage, P. and Cui, Y.J. (2002) “On the high stress compression of bentonites.” Canadian Geotechnical Journal, **39**(4), 812-820.

Martin, R.T. and Ladd, C.C. (1975). “Fabric of consolidated kaolinite.” Clays and Clay Minerals, **23**(1), 17-25.

Mayne, P.W. and Kulhawy, F.H. (1982). “K_0-OCR relationships in soils.” Journal of Geotechnical Engineering, **108**, 851–872.

Mesri, G. and Hayat, T.M. (1993). “The coefficient of earth pressure at rest.” Canadian Geotechnical Journal, **30**(4), 647-666.

Min, T. (2010). “Research on test method of earth pressure at rest for deep soil.” MS Dissertation, China University of Mining and Technology: China (in Chinese).

Okochi, Y. and Tatsuoka, F. (1984). “Some factors affecting K_0 values of sand measured in triaxial 75 cell.” Soils and Foundations, **24**, 52–68.

Pestana, J.M. and Whittle, A.J. (1999). “Formulation of a unified constitutive model for clays and sands”. *International Journal for Numerical and Analytical Methods*, **23**(12), 1215-1243.

Roscoe, K.H., Schofield, A.N. and Wroth, C.P. (1958). “On the Yielding of Soils.” Géotechnique, **8**(1), 22-53.

Schofield, A. and Worth, P. (1968). Critical state soil mechanics. McGraw-Hill: New York.

Shang, X.Y. (2009). “Study on the mechanical properties of deep clay under various stress level.” Ph.D. Dissertation, China University of Mining and Technology: China (in

Chinese).

Shang, X.Y., Yu, H.-S., Zhou, G.Q., Wang, F. and Lu, Y. (2012). “Micro analysis on mechanical characteristics of deep clay under high stress level.” China Journal of Geotechnical Engineering, **34**(2), 363-368 (in Chinese).

Shang, X.Y., Zhou, G.Q., Kuang, L.F. and Cai, W. (2015a). “Compressibility of deep clay in East China subjected to a wide range of consolidation stresses.” Canadian Geotechnical Journal, **52**(2), 244-250.

Shang, X.Y., Zhou, G.Q., Lu, Y. (2015b). “Stress-dependent undrained shear behavior of remolded deep clay in East China.” Journal of Zhejiang University-SCIENCE A (Applied Physics & Engineering), **16**(3), 171-181.

Shin, H. and Santamarina, J.C. (2009). “Mineral dissolution and the evolution of K_0.” Journal of Geotechnical and Geoenvironmental Engineering, ASCE **135**(8), 1141–1147.

Sivasithamparam, N. and Castro, J. (2016). “An anisotropic elastoplastic model for soft clays based on logarithmic contractancy.” International Journal for Numerical and Analytical Methods in Geomechanics, **40**, 596 – 621.

Sjoblom, J.K. (2016). “Coarse-Grained Molecular Dynamics Approach to Simulating Clay Behavior.” Journal of Geotechnical and Geoenvironmental Engineering, **142**(2), 06015013.

Smith, D.W., Narsilio, G.A. and Pivonka, P. (2009). “Numerical particle-scale study of swelling pressure in clays.” KSCE Journal of Civil Engineering, **13**(4), 273-279.

Sui, W.H., Zhang, G.L., and Shen, W. (1994). “High pressure consolidation and secondary consolidation characteristics of deep soil layer in a coal mining area.” Coal Geology & Exploration, **22**(2), 37-40 (in Chinese).

Terzaghi, K. (1920), “Old Earth Pressure Theories and New Test Results”, Engineering News Record, **85**, 632.

Tian, Q.H., Xu, Z.W., Zhou, G.Q., Zhao, X.D. and Hu, K. (2009). “Coefficients of earth pressure at rest in thick and deep soils.” Mining Science and Technology, **19**(2), 252-255.

Ting, C.M.R., Sills, G.C. and Wijeyesekera, D.C. (1994) “Development of K_0 in soft soils.” Géotechnique, 44(1), 101-109.

Wang, C.Y. and Mao, N.H. (1980). “Mechanical properties of clays at high pressure.” Journal of Geophysics Research, **85**(B3), 1462-1468.

Wang, X.Y., Tang, Y.Q., Zang, Y.Z., Chen, J. and Han, S.P. (2007). “Experimental studies and new ideas on the lateral stress in soil.” China Journal of Geotechnical Engineering, **29**(3), 430-435 (in Chinese).

Wheeler, S.J., Naatanen, A., Karstunen, K. and Lojander, M. (2003). “An anisotropic elastoplastic model for soft clays.” Canadian Geotechnical Journal, 40(2):403 – 418.

William, H.P., Brian, P.F., Saul, A.T. and William, T.V. (1997). Numerical recipes in FORTRAN 77-The art of scientific computing. Cambridge University Press: Cambridge.

Wood, D.M. (1990). Soil behaviour and critical state soil mechanics. Cambridge University Press: Cambridge.

Wroth, C.P. (1975), “In Situ Measurements on Initial Stresses and Deformation Characteristics”, Proceedings, In Situ Measurement of Soil Properties, North Carolina State University, Geotechnical Engineering Division, pp. 181-230.

Xu, Z.W., Zheng, K.H., Wei, Z., Liu, Z.Q., Zhao, X.D. and Tian, Q.H. (2009). “Nonlinear characteristics of the static earth pressure coefficient in thick alluvium.” Mining Science and Technology, **19**(1), 129-132.

Yamamuro, J.A., Bopp, P.A. and Lade, P.V. (1996). “One-dimensional compression of sands at high pressure.” Journal of Geotechnical Engineering, **22**(2), 147-154.

Yao, X.L., Qi, J.L. and Yu, F. (2014). “Study on lateral earth pressure coefficient at rest for frozen soils.” Journal of Offshore Mechanics and Arctic Engineering, **136**(1), 011301.

Yu, H.-S. (1998), “CASM: A unified sate parameter model for clay and sand.” International Journal for Numerical and Analytical Methods in Geomechanics, **22**, 621-653.

Yu, H.-S. (2006). Plasticity and geotechnics. Springer-Verlag: New York.

Figure1

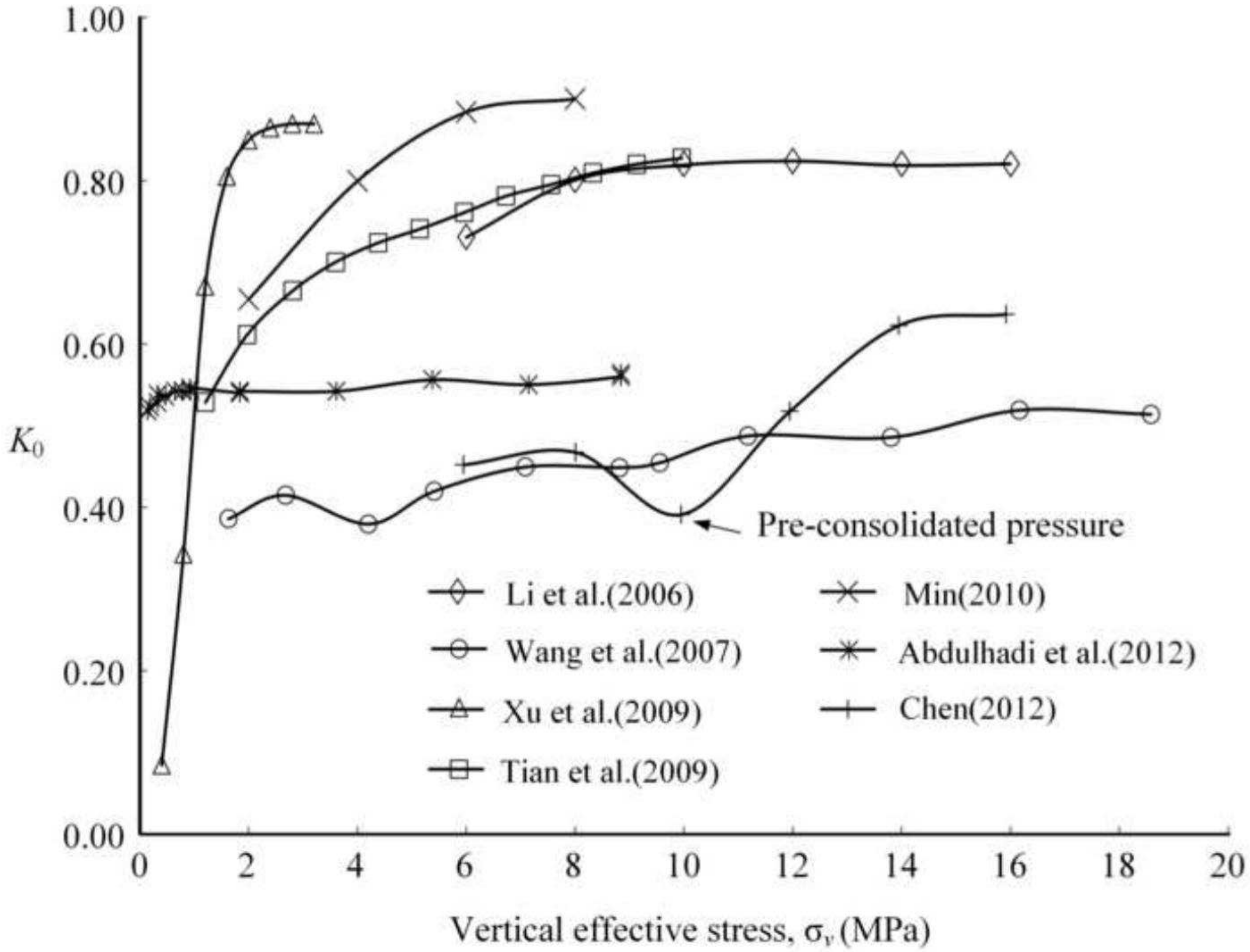
1.00
0.80
0.60
0.40
0.20
0.00
K_0
0
2
4
6
8
10
12
14
16
18
20
Vertical effective stress, σ_v (MPa)
Pre-consolidated pressure
Li et al.(2006)
Wang et al.(2007)
Xu et al.(2009)
Tian et al.(2009)
Min(2010)
Abdulhadi et al.(2012)
Chen(2012)

Figure2

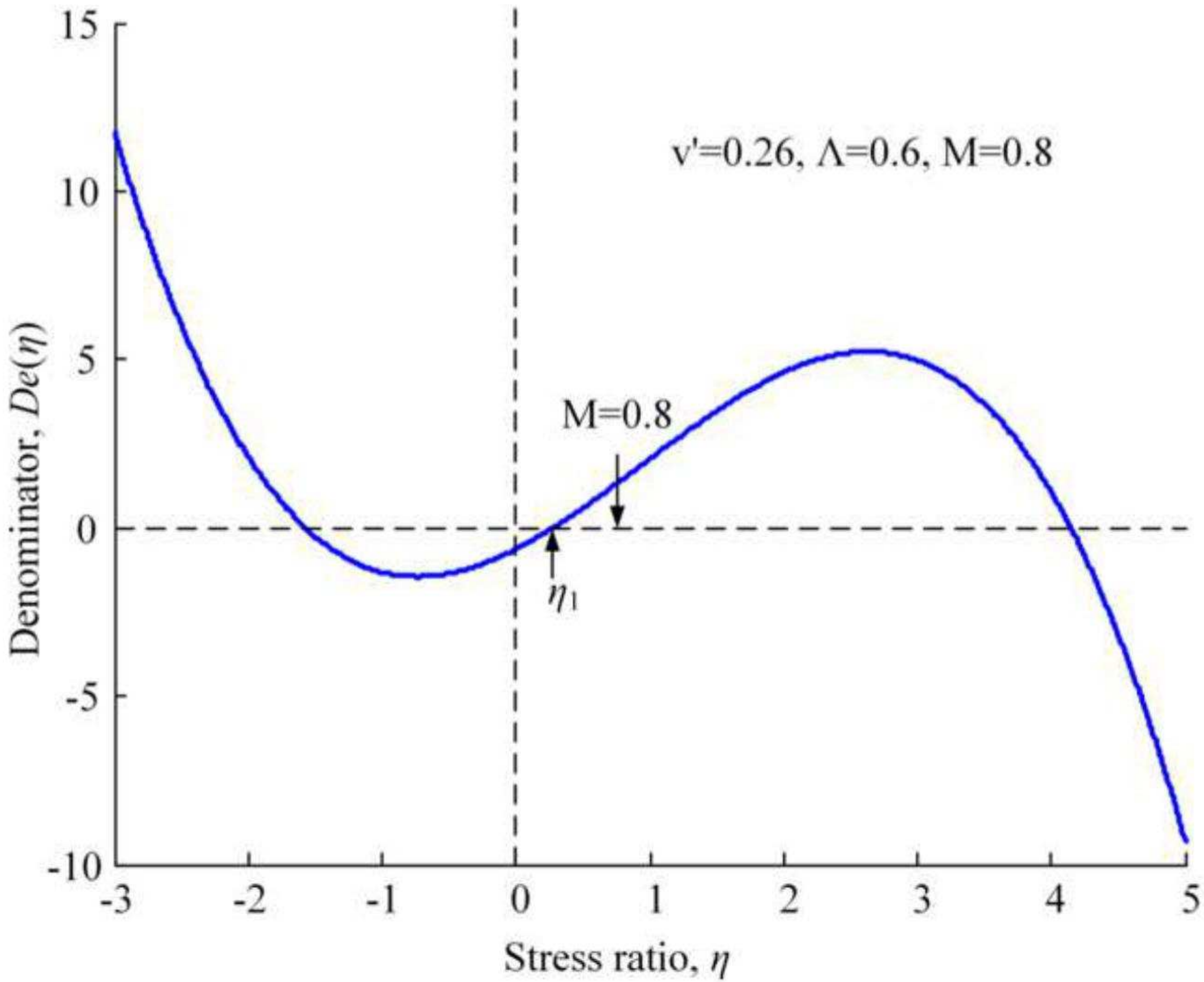
v'=0.26, Λ=0.6, M=0.8
M=0.8
η1
Denominator, De(η)
Stress ratio, η
15
10
5
0
-5
-10
-3
-2
-1
0
1
2
3
4
5

Figure3.a

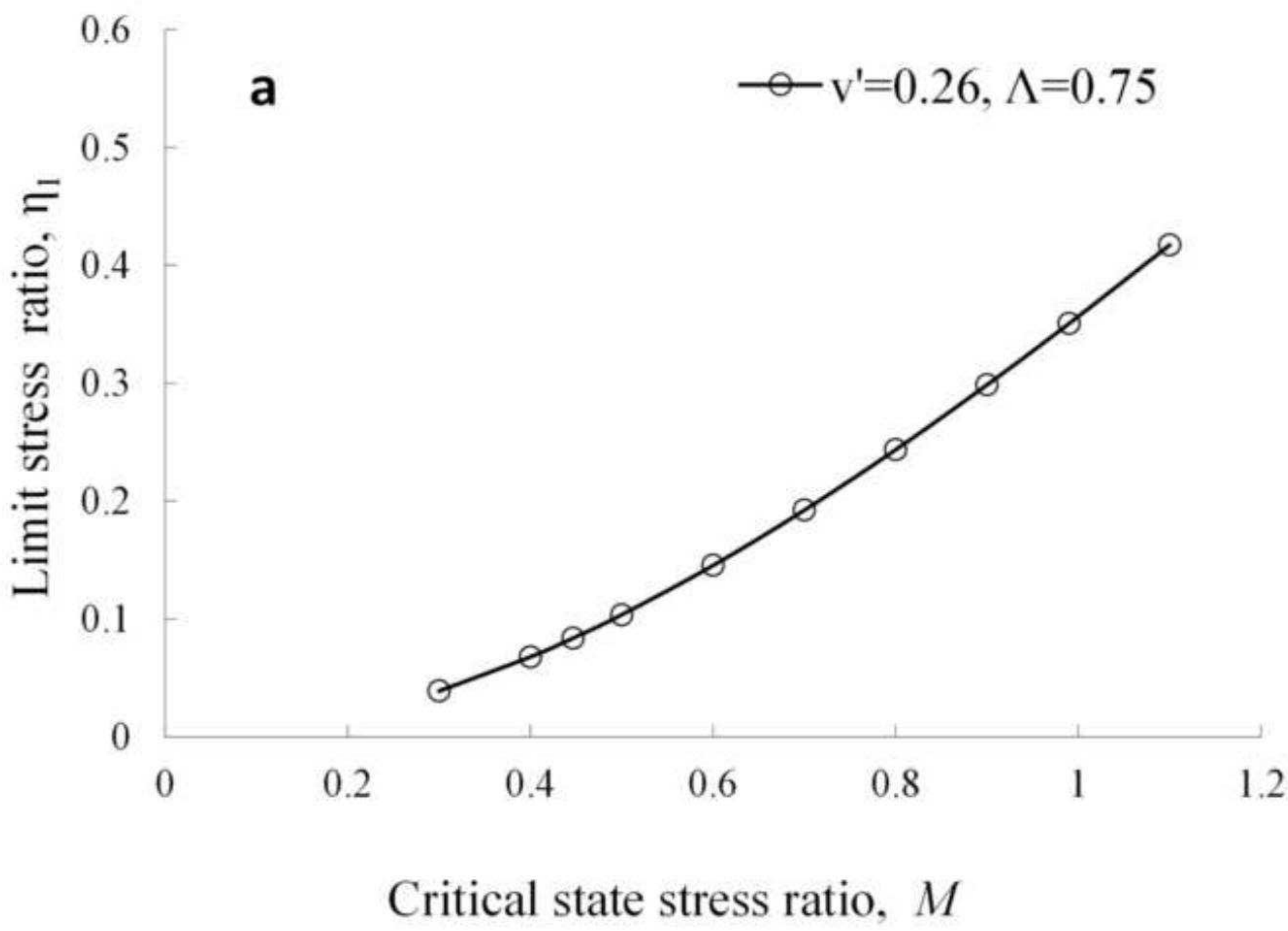
a
v'=0.26, Λ=0.75
Limit stress ratio, η_l
Critical state stress ratio, M
0
0.1
0.2
0.3
0.4
0.5
0.6
0
0.2
0.4
0.6
0.8
1
1.2

Figure3.b

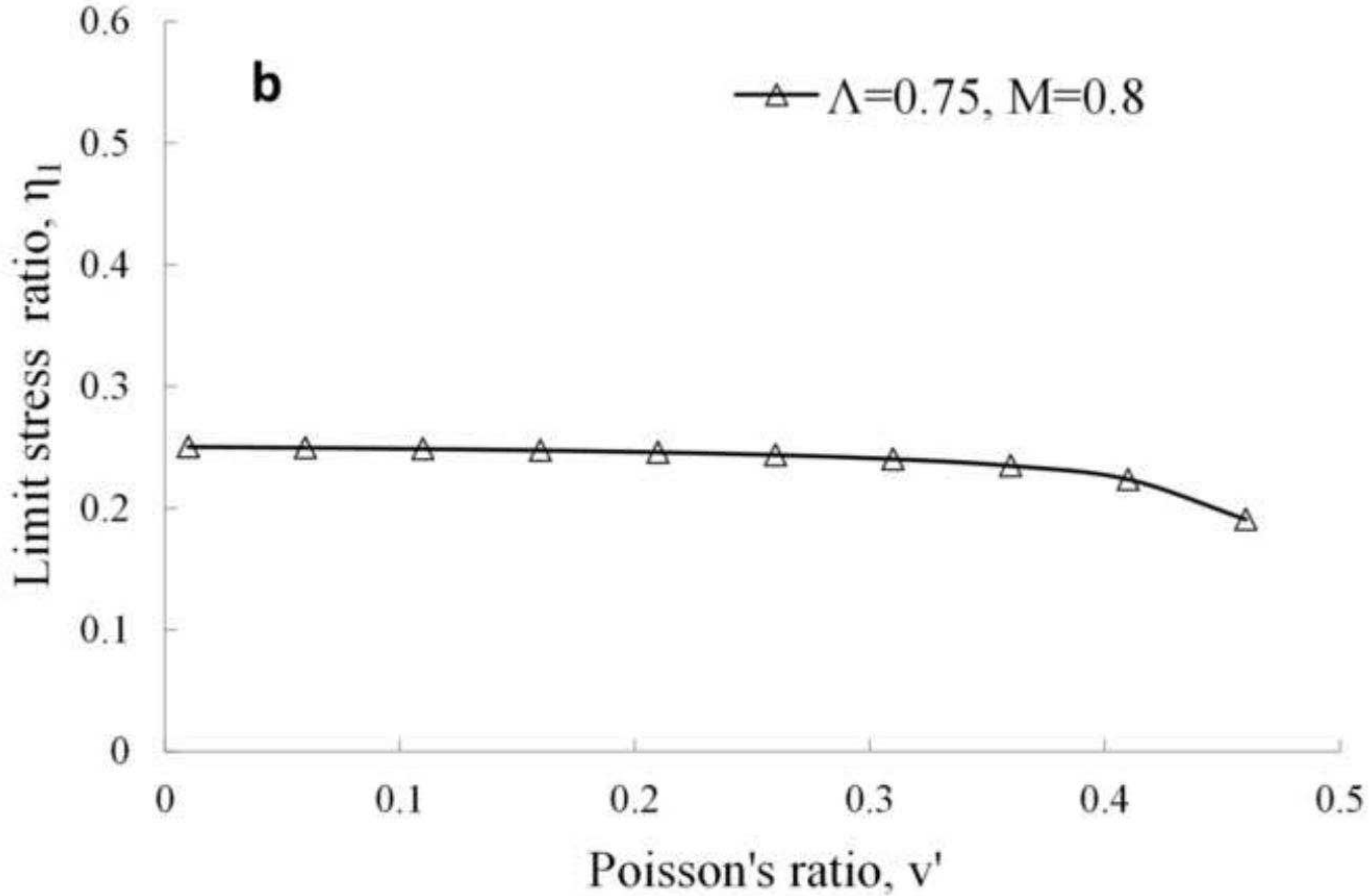

b
Λ=0.75, M=0.8
0.6
0.5
0.4
0.3
0.2
0.1
0
Limit stress ratio, η1
0
0.1
0.2
0.3
0.4
0.5
Poisson's ratio, v'

Figure3.c

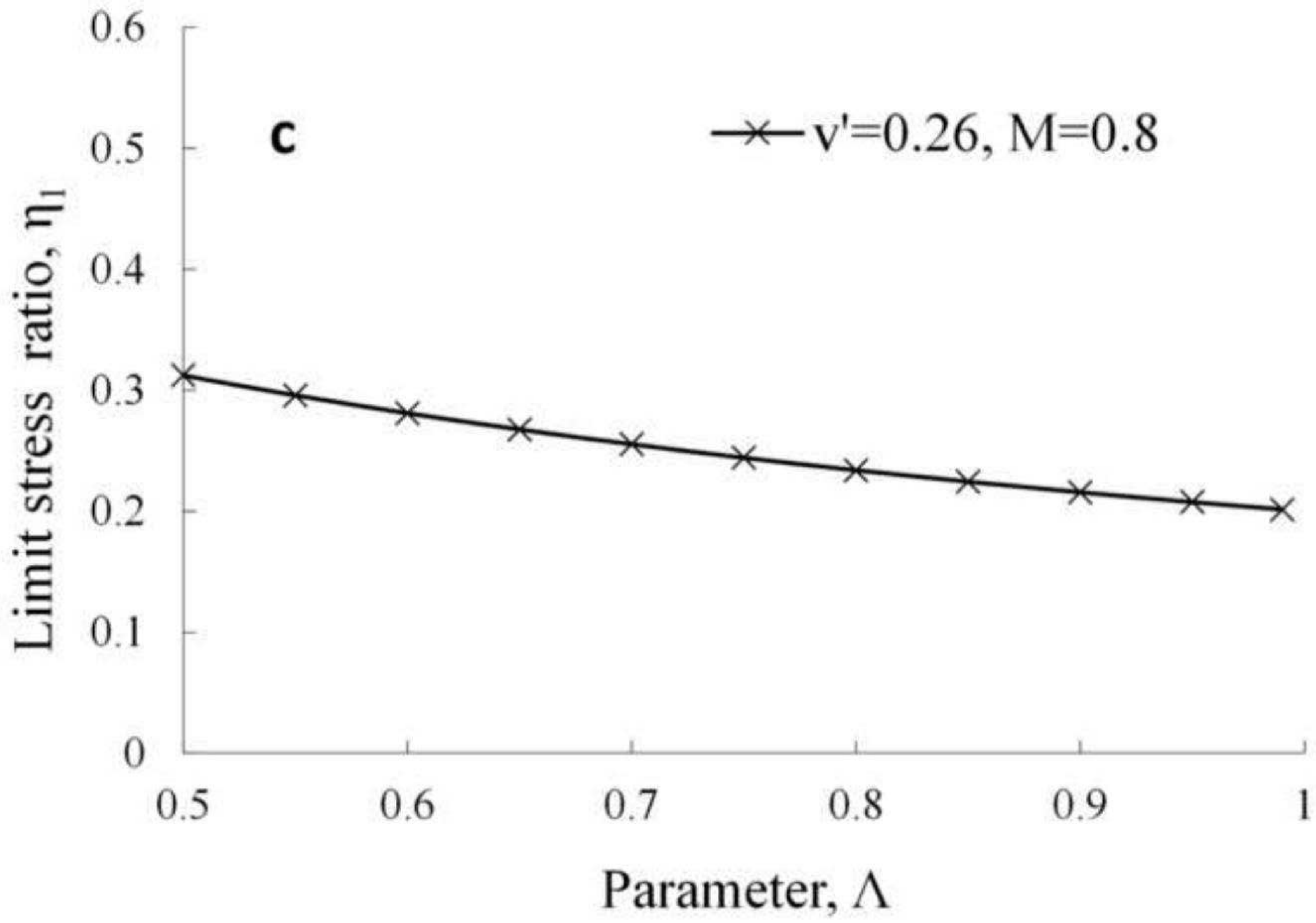
c
v'=0.26, M=0.8
Limit stress ratio, η1
0.6
0.5
0.4
0.3
0.2
0.1
0
0.5
0.6
0.7
0.8
0.9
1
Parameter, Λ

Figure4

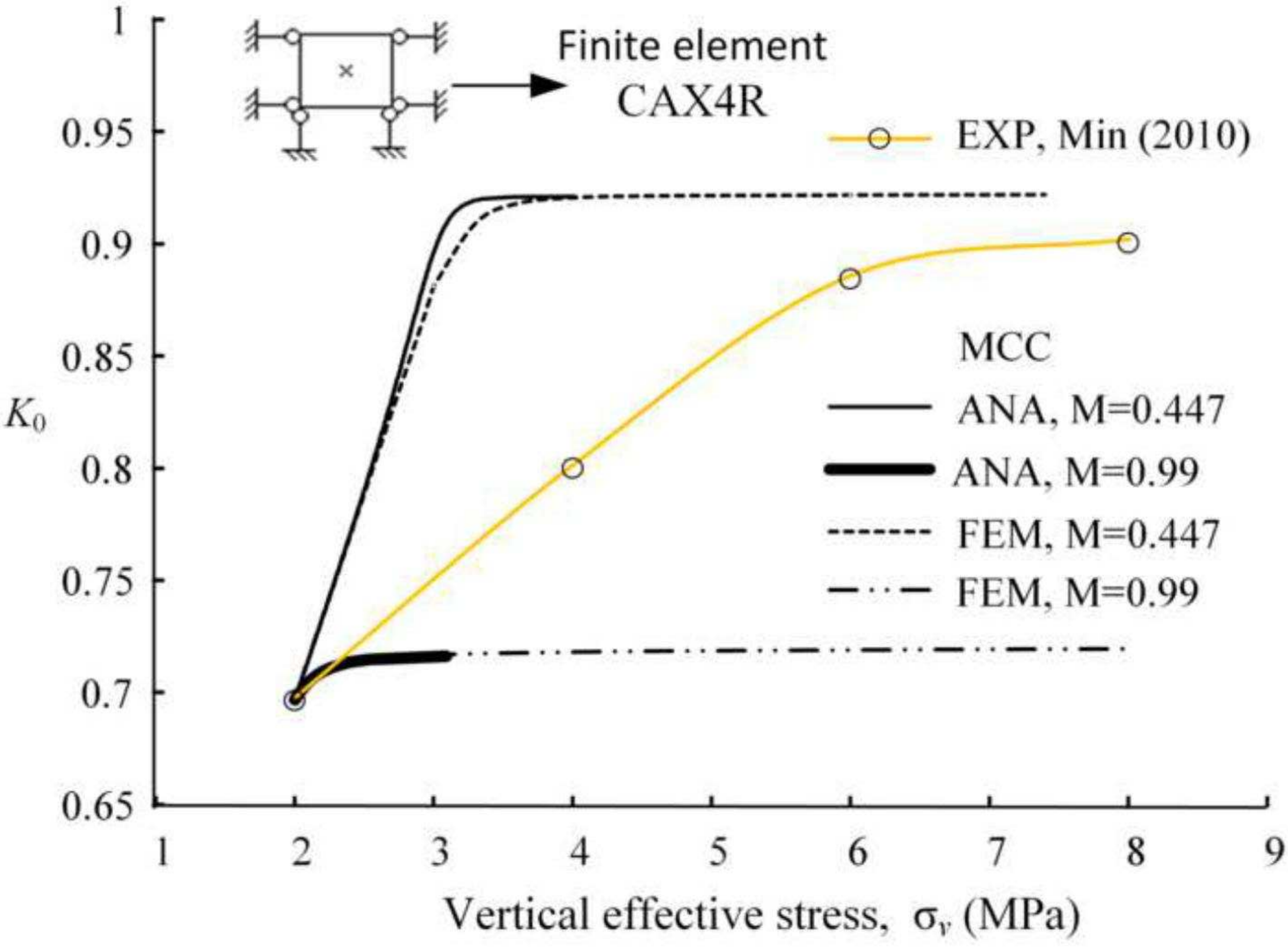
Finite element
CAX4R
EXP, Min (2010)
MCC
ANA, M=0.447
ANA, M=0.99
FEM, M=0.447
FEM, M=0.99
K_0
1
0.95
0.9
0.85
0.8
0.75
0.7
0.65
1
2
3
4
5
6
7
8
9
Vertical effective stress, σ_v (MPa)

Figure5

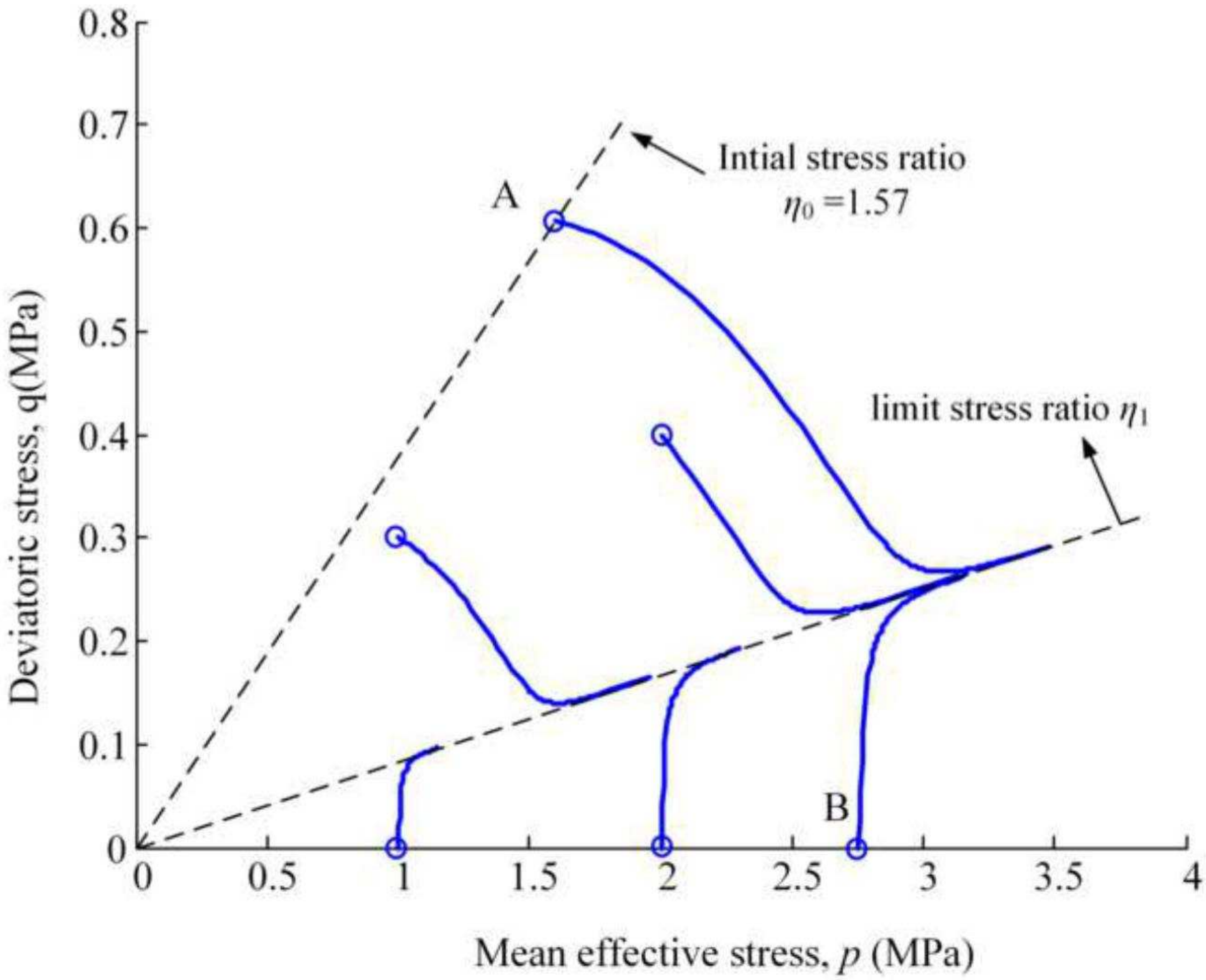

Intial stress ratio
η_0 =1.57
limit stress ratio η_1
A
B
0.8
0.7
0.6
0.5
0.4
0.3
0.2
0.1
0
0
0.5
1
1.5
2
2.5
3
3.5
4
Deviatoric stress, q(MPa)
Mean effective stress, p (MPa)

Figure6.a

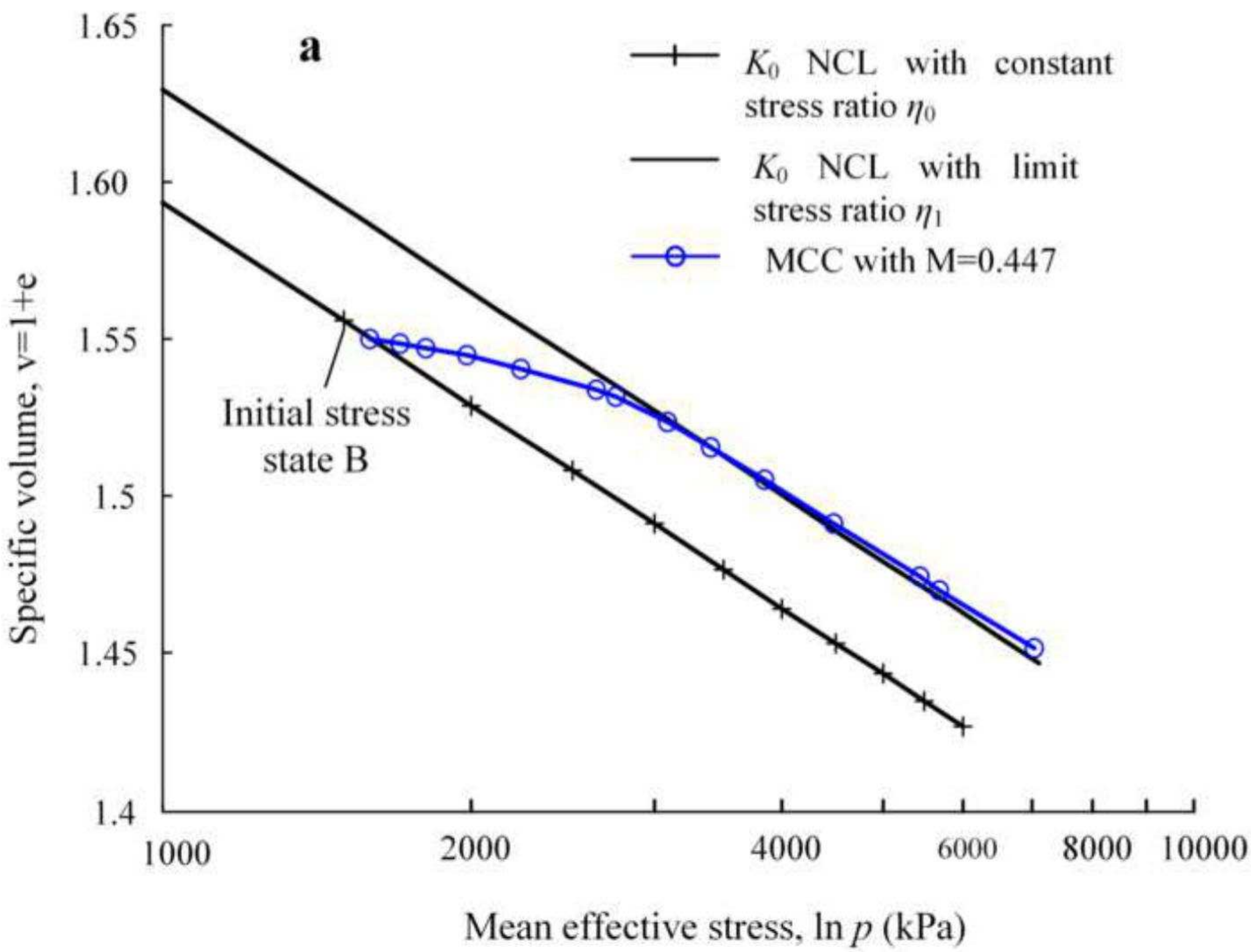
a
K_0 NCL with constant stress ratio η_0
K_0 NCL with limit stress ratio η_1
MCC with M=0.447
Initial stress state B
Specific volume, v=1+e
1.65
1.60
1.55
1.5
1.45
1.4
1000
2000
4000
6000
8000
10000
Mean effective stress, ln p (kPa)

Figure6.b

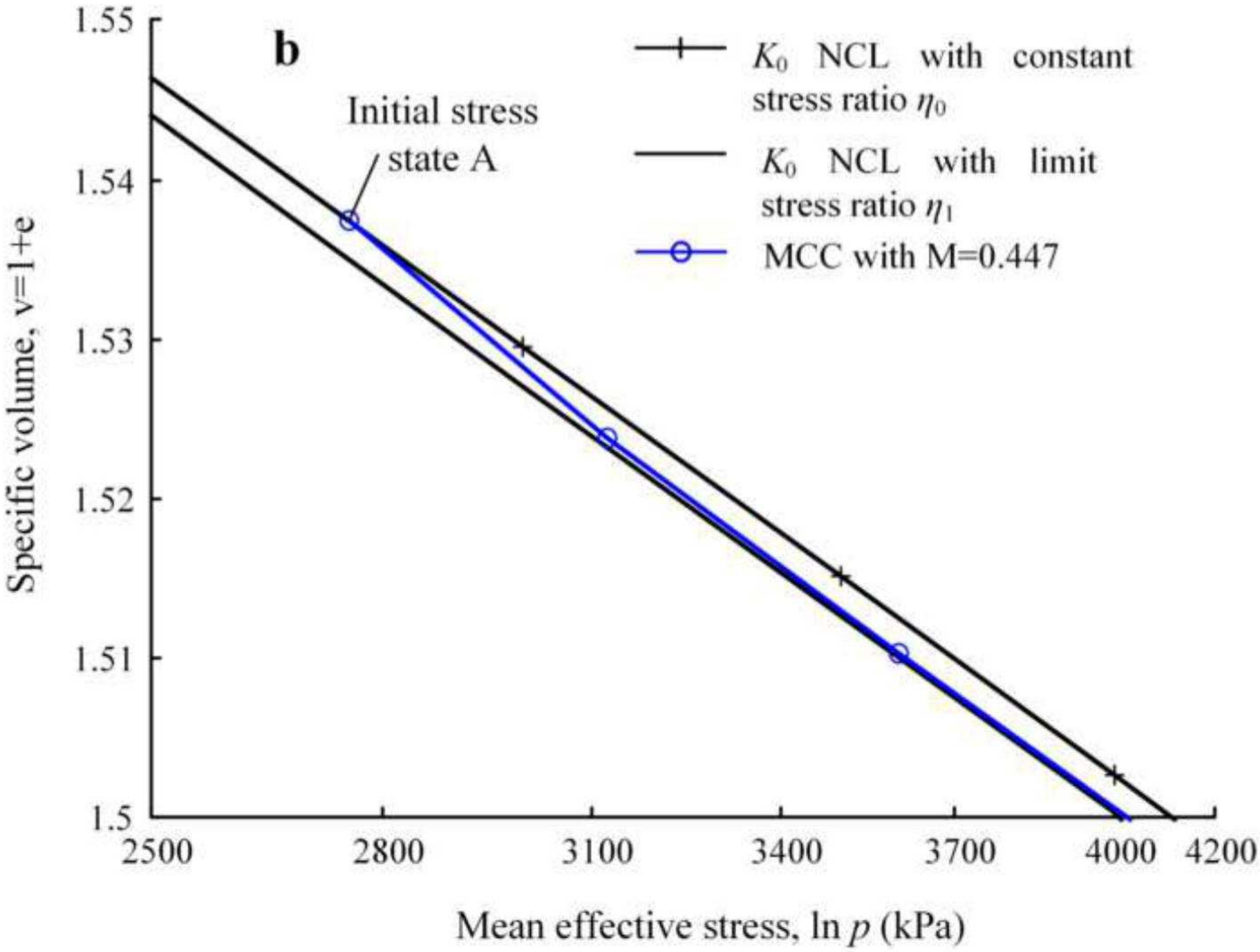
b
Initial stress
state A
K_0 NCL with constant stress ratio η_0
K_0 NCL with limit stress ratio η_1
MCC with M=0.447
1.55
1.54
1.53
1.52
1.51
1.5
2500
2800
3100
3400
3700
4000
4200
Specific volume, v=1+e
Mean effective stress, ln p (kPa)

Figure7.a

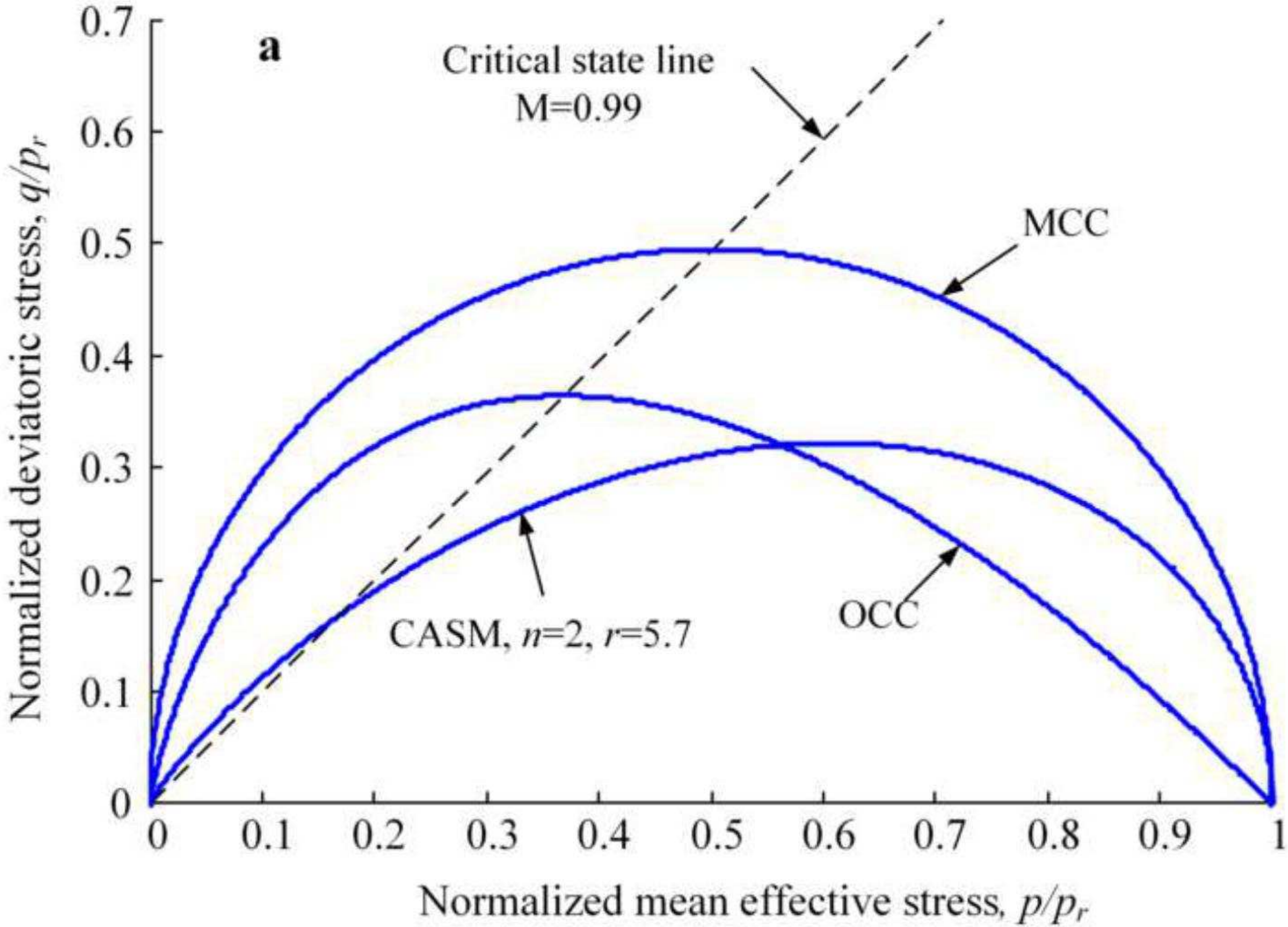
a
Critical state line
M=0.99
MCC
OCC
CASM, n=2, r=5.7
Normalized deviatoric stress, q/p_r
Normalized mean effective stress, p/p_r
0
0.1
0.2
0.3
0.4
0.5
0.6
0.7
0.8
0.9
1

Figure7.b

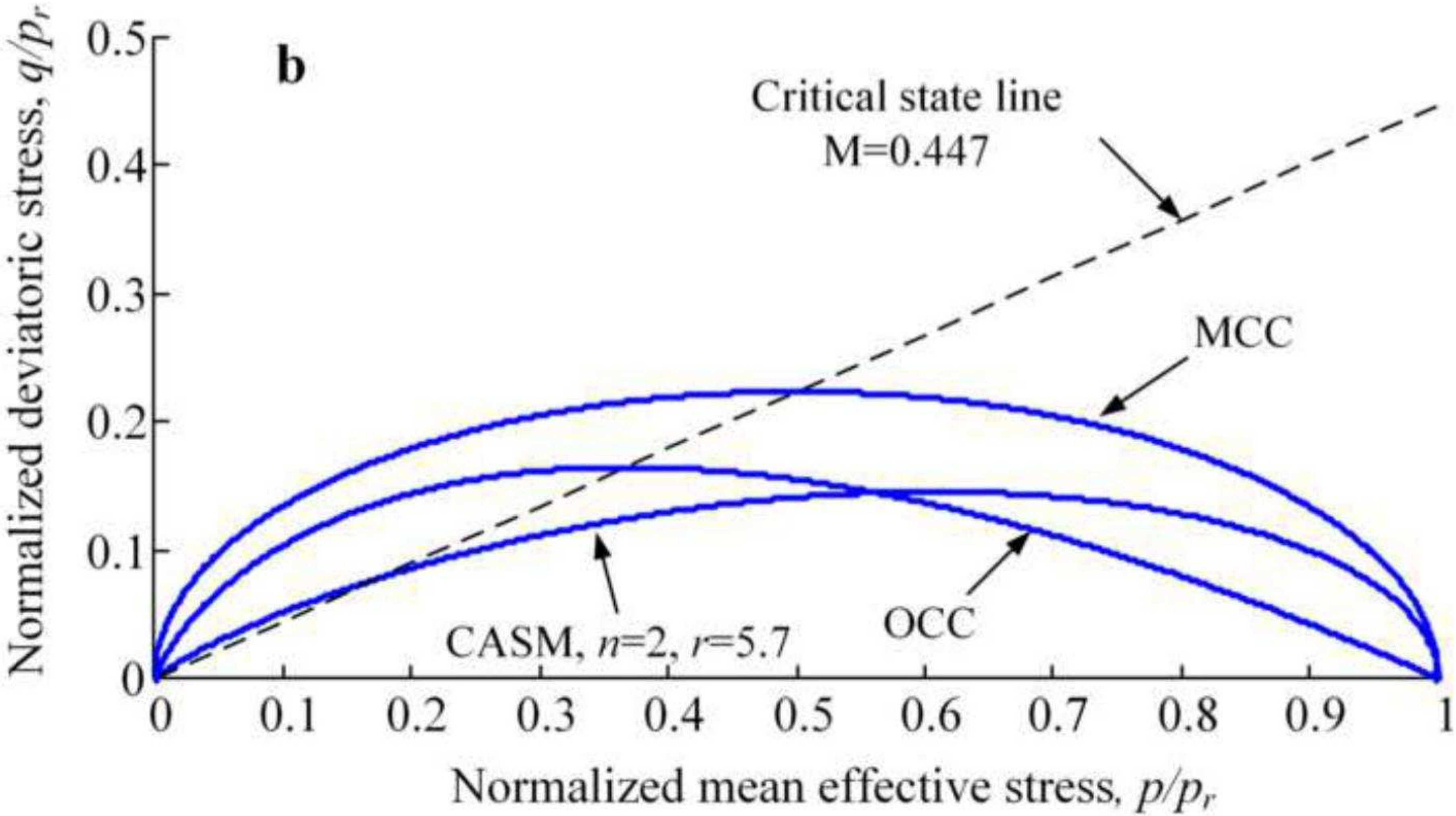
b
Critical state line
M=0.447
MCC
OCC
CASM, n=2, r=5.7
Normalized deviatoric stress, q/p_r
Normalized mean effective stress, p/p_r
0
0.1
0.2
0.3
0.4
0.5
0.6
0.7
0.8
0.9
1

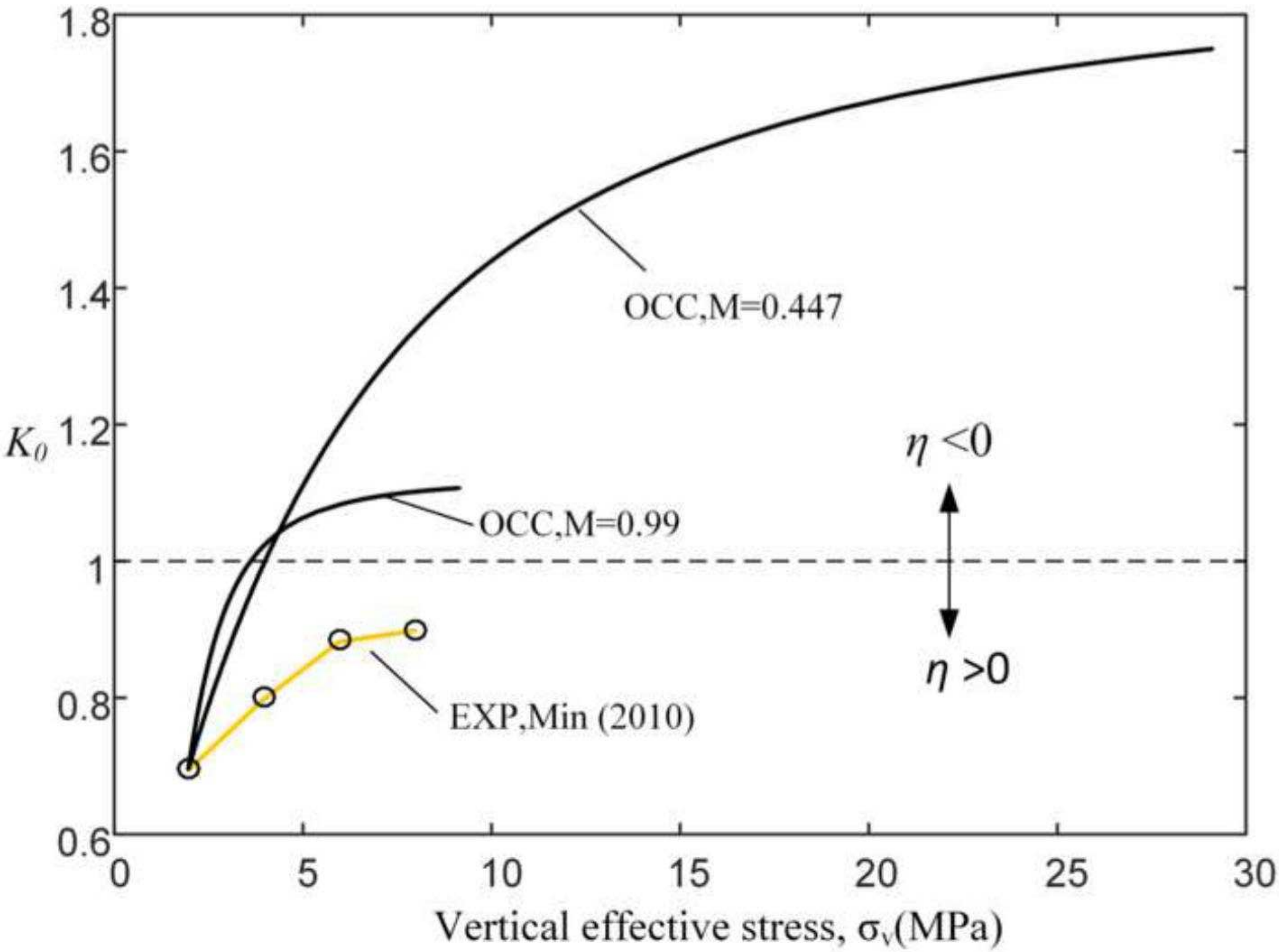
1.8
1.6
1.4
1.2
1
0.8
0.6
K_0
0
5
10
15
20
25
30
Vertical effective stress, σ_v(MPa)
OCC,M=0.447
OCC,M=0.99
EXP,Min (2010)
η <0
η >0

Figure9

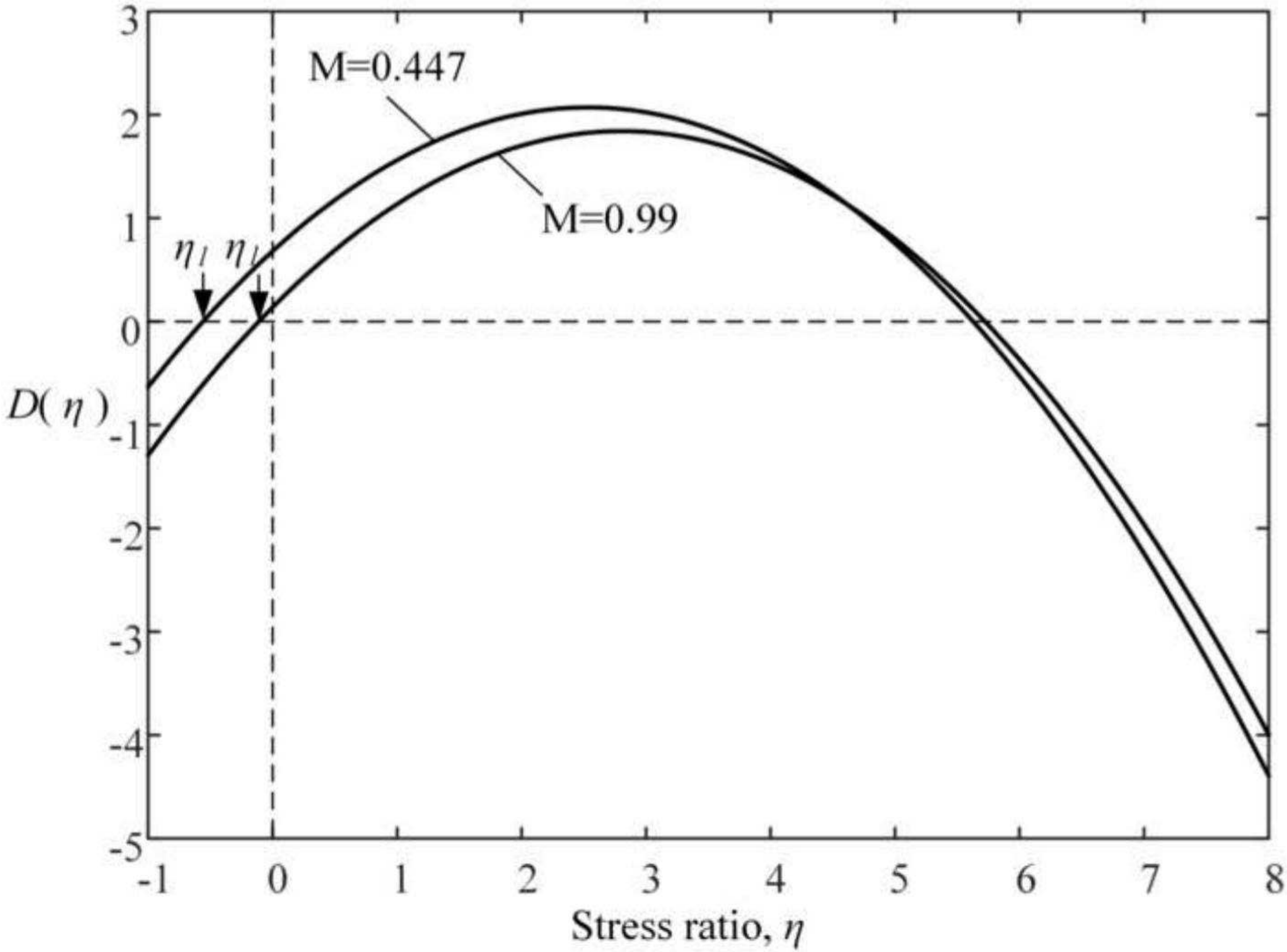
M=0.447
M=0.99
η_l η_l
$D(\eta)$
Stress ratio, η
3
2
1
0
-1
-2
-3
-4
-5
-1
0
1
2
3
4
5
6
7
8

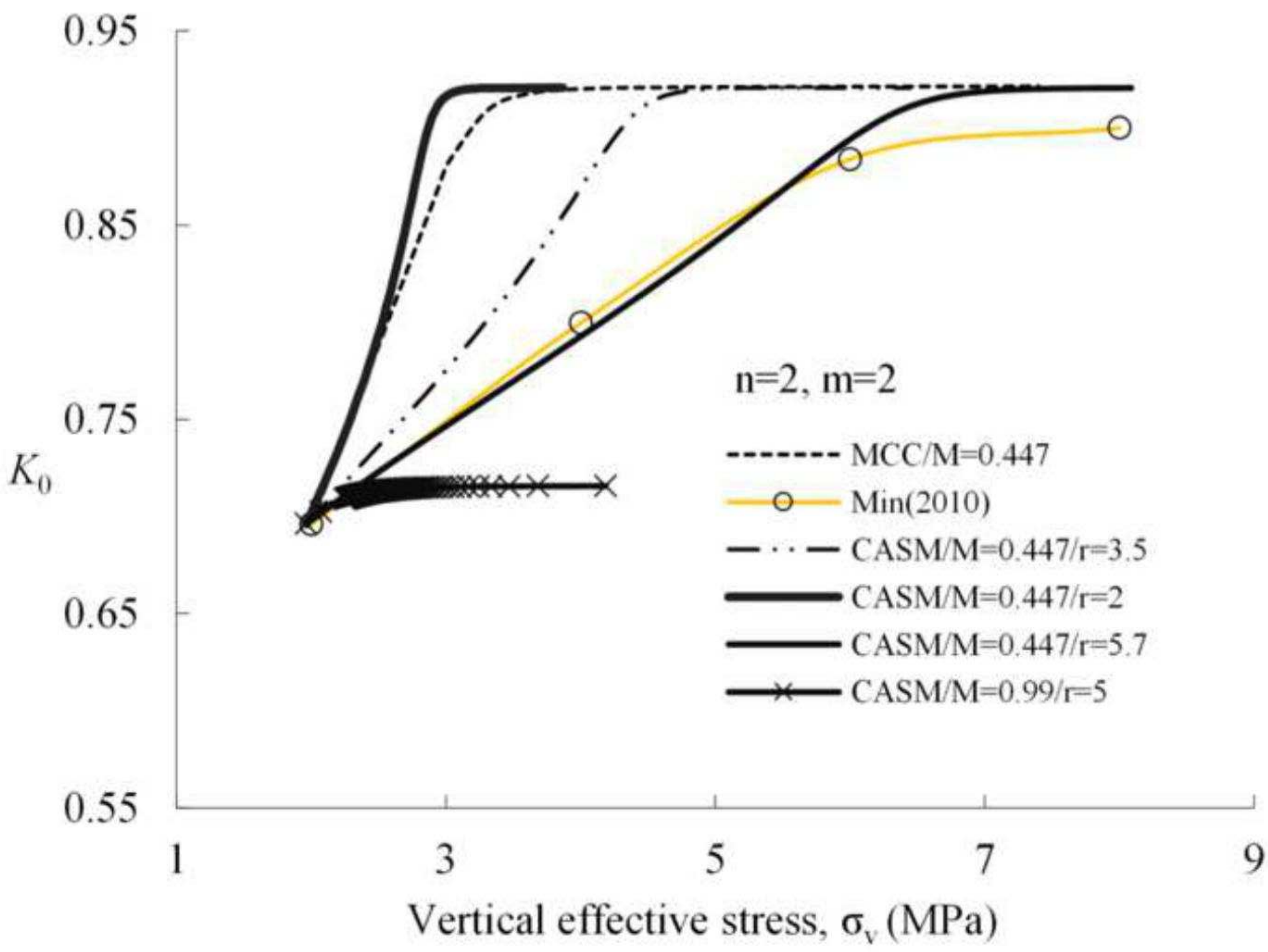
0.95
0.85
0.75
0.65
0.55
K0
1
3
5
7
9
Vertical effective stress, σv (MPa)
n=2, m=2
MCC/M=0.447
Min(2010)
CASM/M=0.447/r=3.5
CASM/M=0.447/r=2
CASM/M=0.447/r=5.7
CASM/M=0.99/r=5

Figure11

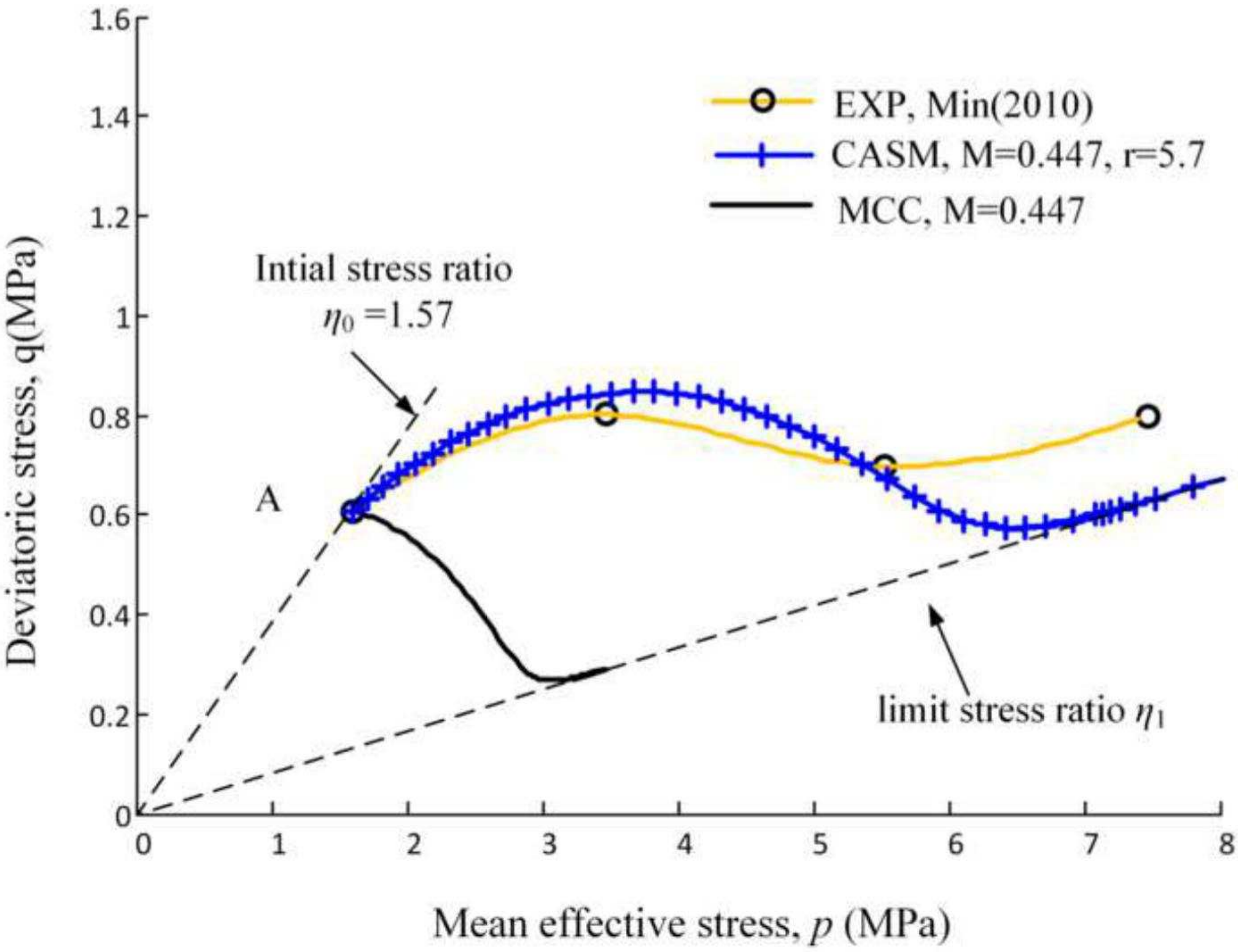
EXP, Min(2010)
CASM, M=0.447, r=5.7
MCC, M=0.447
Intial stress ratio
η_0 =1.57
A
limit stress ratio η_1
Deviatoric stress, q(MPa)
Mean effective stress, p (MPa)
0
0.2
0.4
0.6
0.8
1
1.2
1.4
1.6
0
1
2
3
4
5
6
7
8